

**SUBSURFACE FLOW MANAGEMENT AND REAL-TIME PRODUCTION
OPTIMIZATION USING MODEL PREDICTIVE CONTROL**

A Thesis

by

THOMAS JAI LOPEZ

Submitted to the Office of Graduate Studies of
Texas A&M University
in partial fulfillment of the requirements for the degree of

MASTER OF SCIENCE

December 2011

Major Subject: Petroleum Engineering

**SUBSURFACE FLOW MANAGEMENT AND REAL-TIME PRODUCTION
OPTIMIZATION USING MODEL PREDICTIVE CONTROL**

A Thesis

by

THOMAS JAI LOPEZ

Submitted to the Office of Graduate Studies of
Texas A&M University
in partial fulfillment of the requirements for the degree of

MASTER OF SCIENCE

Approved by:

Chair of Committee,	Eduardo Gildin
Committee Members,	Akhil Datta Gupta
	Won-jong Kim
Head of Department,	Stephen A. Holditch

December 2011

Major Subject: Petroleum Engineering

ABSTRACT

Subsurface Flow Management and Real-Time Production Optimization Using Model
Predictive Control. (December 2011)

Thomas Jai Lopez, B.E., Birla Institute of Science and Technology

Chair of Advisory Committee: Dr. Eduardo Gildin

One of the key challenges in the Oil & Gas industry is to best manage reservoirs under different conditions, constrained by production rates based on various economic scenarios, in order to meet energy demands and maximize profit. To address the energy demand challenges, a transformation in the paradigm of the utilization of “real-time” data has to be brought to bear, as one changes from a static decision making to a dynamical and data-driven management of production in conjunction with real-time risk assessment. The use of modern methods of computational modeling and simulation may be the only means to account for the two major tasks involved in this paradigm shift: (1) large-scale computations; and (2) efficient utilization of the deluge of data streams.

Recently, history matching and optimization were brought together in the oil industry into an integrated and more structured approach called optimal closed-loop reservoir management. Closed-loop control algorithms have already been applied extensively in other engineering fields, including aerospace, mechanical, electrical and chemical engineering. However, their applications to porous media flow, such as - in the current practices and improvements in oil and gas recovery, in aquifer management, in

bio-landfill optimization, and in CO₂ sequestration have been minimal due to the large-scale nature of existing problems that generate complex models for controller design and real-time implementation. Their applicability to a realistic field is also an open topic because of the large-scale nature of existing problems that generate complex models for controller design and real-time implementation, hindering its applicability.

Basically, three sources of high-dimensionality can be identified from the underlying reservoir models: size of parameter space, size of state space, and the number of scenarios or realizations necessary to account for uncertainty. In this paper we will address type problem of high dimensionality by focusing on the mitigation of the size of the state-space models by means of model-order reduction techniques in a systems framework. We will show how one can obtain accurate reduced order models which are amenable to fast implementations in the closed-loop framework. The research will focus on System Identification (System-ID) (Jansen, 2009) and Model Predictive Control (MPC) (Gildin, 2008) to serve this purpose.

A mathematical treatment of System-ID and MPC as applied to reservoir simulation will be presented. Linear MPC would be studied on two specific reservoir models after generating low-order reservoir models using System-ID methods. All the comparisons are provided from a set of realistic simulations using the commercial reservoir simulator called Eclipse®. With the improvements in oil recovery and reductions in water production effectively for both the cases that were considered, we could reinforce our stance in proposing the implementation of MPC and System-ID towards the ultimate goal of “real time” production optimization.

DEDICATION

To my parents

TABLE OF CONTENTS

	Page
ABSTRACT	iii
DEDICATION.....	v
TABLE OF CONTENTS.....	vi
LIST OF FIGURES	viii
LIST OF TABLES.....	x
1. INTRODUCTION	1
1.1 Overview	1
1.2 The Concept of Closed-Loop Control.....	4
1.3 Problems with Large-Scale Systems and Model Order Reduction	10
1.3.1 White Box.....	15
1.3.2 Black Box	20
1.4 Objectives of the Proposed Research	21
2. RESERVOIR SIMULATION AND PRODUCTION OPTIMIZATION	24
2.1 Introduction to Porous Media Flow	24
2.2 Partial Differential Equations	24
2.3 Formulation into Controls Framework	29
2.4 Introduction to Reservoir Simulation – Solution Methods	37
3. INTRODUCTION TO MODEL PREDICTIVE CONTROL	39
3.1 The Basic Formulation.....	40
3.2 The Cost Function.....	42
3.3 The Constraints.....	42
4. INTRODUCTION TO SYSTEM IDENTIFICATION	44
4.1 The Black Box Model.....	45
4.2 An Overview of the Theory.....	46
4.3 An Example - 2D Homogeneous Reservoir	51

	Page
4.3.1 Experimental Design.....	52
4.3.2 Model Validation	57
4.3.3 An Expanded Model	58
5. MPC AND SYSTEM-ID – APPLIED TO RESERVOIR SIMULATION	60
5.1 The Dynamic Control Capability.....	62
5.2 The Formulation of the MPC Control Problem.....	69
5.3 Operational Aspects	73
6. MPC AND SYSTEM-ID – CASE STUDIES AND CONCLUSIONS.....	75
6.1 Case 1 – The Five Spot 2D Reservoir.....	75
6.1.1 Performance Enhancement Using MPC.....	81
6.1.2 The Identification.....	82
6.1.3 Results before Water Breakthrough.....	85
6.1.4 The Big Picture	88
6.2 Case 2 – A Fine Grid Geostatistically Generated Field	93
6.2.1 Reservoir Model Description	93
6.2.2 Well Placement.....	94
6.2.3 Model Dynamics.....	98
6.2.4 MPC Implementation.....	99
6.3 Conclusions	104
6.4 Research Gaps	106
REFERENCES	108
VITA.....	112

LIST OF FIGURES

	Page
Figure 1-1 Block Diagram for Open-Loop Reservoir Management	9
Figure 1-2 Block Diagram for Closed-loop Reservoir Management	9
Figure 1-3 Model Order Reduction Techniques.....	15
Figure 2-1 Grid Cell Transmissibility	27
Figure 3-1 Receding Horizon Principle	41
Figure 4-1 Schematic of Black Box Model.....	45
Figure 4-2 2D Homogeneous Reservoir	51
Figure 4-3 Staircase Experiment	54
Figure 4-4 Input Signal	55
Figure 4-5 Output Obtained	55
Figure 4-6 Simulation Fit	56
Figure 4-7 Model Validation Fit.....	57
Figure 4-8 Expanded Model Fit.....	58
Figure 5-1 Open-Loop Waterflooding	60
Figure 5-2 Proposed Controller for Waterflooding	61
Figure 5-3 MPC as Applied to Waterflooding Control - a	63
Figure 5-4 MPC as Applied to Waterflooding Control - b	64
Figure 5-5 MPC as Applied to Waterflooding Control - c.....	65
Figure 5-6 MPC as Applied to Waterflooding Control - d	66
Figure 5-7 MPC as Applied to Waterflooding Control - e.....	67

	Page
Figure 5-8 MPC as Applied to Waterflooding Control - f	68
Figure 6-1 Homogeneous Reservoir for Case 1	76
Figure 6-2 Phase Rates for Homogeneous Reservoir	78
Figure 6-3 Homogeneous Reservoir with High-Perm Channel for Case 1	79
Figure 6-4 Open-loop Phase Rates for Homogeneous Reservoir with Channel	80
Figure 6-5 Simulation Fit for Homogeneous Reservoir with Channel	83
Figure 6-6 Expanded Simulation Fit for Homogeneous Reservoir with Channel	84
Figure 6-7 MPC Inputs – BHP for Homogeneous Reservoir with Channel	86
Figure 6-8 MPC Outputs for Homogeneous Reservoir with Channel	87
Figure 6-9 MPC Inputs –Rates for Homogeneous Reservoir with Channel	88
Figure 6-10 MPC Optimized Lifecycle Production Phase Rates – Case 1	89
Figure 6-11 MPC Optimized Lifecycle Cumulative Production – Case 1	92
Figure 6-12 Reservoir Model for Case 2.....	94
Figure 6-13 Porosity and Permeability Field for Case 2.....	95
Figure 6-14 Simulation Fit for Case 2	97
Figure 6-15 MPC Optimized Open-Loop and Closed-Loop Phase Rates – Well 5	100
Figure 6-16 MPC Optimized Open-Loop and Closed-Loop Phase Rates – Well 1	102
Figure 6-17 MPC Optimized Open-Loop and Closed-Loop Phase Rates – Well 2	102
Figure 6-18 MPC Optimized Open-Loop and Closed-Loop Phase Rates – Well 3	103
Figure 6-19 MPC Optimized Open-Loop and Closed-Loop Phase Rates – Well 4	103
Figure 6-20 MPC Optimized Lifecycle Cumulative Production – Case 2	104

LIST OF TABLES

	Page
Table 1-1 Example to Illustrate State-Space Formulation	33
Table 4-1 Reservoir and Fluid Properties for System-ID	52
Table 6-1 Reservoir and Fluid Properties for Case 1	76
Table 6-2 Reservoir and Fluid Properties for Case 2	96

1. INTRODUCTION

1.1 Overview

Imagine planning and implementing the evacuation of a crowded city- on a moonless night, from a helicopter. We may have a basic idea of the road layout and some understanding of how the towns are generally planned and some old scrap of local information. But there might just be a few streetlamps that are switched on and we are working in darkness. Producing oil and gas from a reservoir is very similar in nature wherein the well can be compared to be the streetlamp illuminating its very immediate surroundings, but nothing more. The information we receive from seismic interpretation of the geology would serve as the sketchy plan of the reservoir. But as reservoir engineers our job is to come up with a plan to squeeze out as much oil as possible, though we are basically working in the dark.

The knowledge of geology and science has given us enough rules of thumb to make reasonable assumptions of what might be down there in the reservoirs, but as engineers, we still need to make that million-dollar decision based on incredibly small amounts of hard information. How could we go from surveying dunes in desert or waves on the ocean to the point of being prepared to spend millions of dollars finding out what lies beneath it.

It has always been an empirical process. Like any scientific process, we have to act on our theory, test it, then get the results, interpret them and intervene to optimize our plan. But when it comes to exploration and production, there is always a degree of risk and uncertainty that we have to live with all the time. It is this risk associated with the industry that makes reservoir simulation and well test analysis all the more challenging. Once a well has been drilled for exploration, we perform well testing to listen to how the reservoir responds and adapt to events. Reservoir simulation on the other hand has been used as a predictive tool that has gradually become a standard in the petroleum industry. Its widespread acceptance in the recent past could be attributed to the following:

- Advances in computing (particularly the increase in computer memory/storage and in the speed of computation).
- Advances in reservoir characterization techniques.
- Advances in numerical techniques for solving the partial differential equations that govern the reservoir model.
- The generality built into reservoir simulators which make them useful in modeling field cases especially complicated oil-recovery techniques that would otherwise be impossible to analyze.

Reservoir simulators have thus made use of this high speed computing facilities quite effectively. They utilize the computational power to solve the set of algebraic mathematical equation developed from a set of partial differential equations that describe the physical behavior of the process in a reservoir to obtain a numerical solution for the reservoir behavior in the field. These mathematical equations would

account for the most important physical processes taking place in the reservoir including the complex dynamics of the fluids partitioned into as many as three phases (oil water and gas) and the mass transfer between the three phases. In addition to these effects, the mass transfer between the various phases, viscous, gravity and capillary effects on the fluid flow are also taken into consideration. Furthermore, the spatial variations of rock properties, fluid properties, and relative permeability information can be represented with a great amount of details in the reservoir simulator [1].

However the size of the large scale system whose complexity we wish to model in our reservoir simulators has always raised additional challenges from a system and controls perspective. Given the economic importance in depleting the reservoir in the most optimal way, there is a serious challenge of rationalizing the complete decision making process. For this reason, in recent years, a fresh look at how real-time data may be integrated in the decision-making process and in the creation of value in the Oil & Gas industry has opened new avenues of research and, in turn, a new set of challenges have been put forth.

Smart wells, e-field, i-fields, among other ideas were developed based on the premise that real-time data, field-wide optimization and parameter estimation (history matching) could be put together in a somewhat structured manner, called closed loop reservoir management. Large investments were made to deploy computers, sensors and actuators all over the field, ensuring continuous real-time influx of data. It is well disseminated in the industry that worldwide spending on the technological infrastructures for real time-data are ineffective unless value is created by utilizing the

improved knowledge and information that these investments provide. The challenge is to bring about substantial improvement in developing software and work processes that can help us cope with this data flux. Therefore, we need to ensure that the control and optimization decisions are made more rapidly so that the “real time” nature of the smart wells is not lost.

Real time control and optimization appear to be impractical since reservoir models are highly non-linear and have a large number of parameters and states, and thus require large amount of computational power. In many cases, the underlying model used to solve the forward problem in an optimization or in an inverse modeling scheme (parameter estimation) is a product of discretization of a set of partial differential equations (PDE's). Hence, highly accurate and detailed description of the underlying models induce dynamical systems of large dimensions either in the state or parameter spaces (several millions of grid blocks are often obtained). Recent studies, however, show that from an input-output perspective, fairly simple models are preferable over complex ones. In this case, the speed of computations is greatly improved without penalizing the accuracy of the solutions.

1.2 The Concept of Closed-Loop Control

The production phase of hydrocarbon recovery process has been carried out for a long time in an open-loop fashion as shown in Figure 1-1. The exploration and production phases in the hydrocarbon recovery process starts by what we call the field development. Field development basically involves the various steps and processes

involved in identifying an economically beneficial reservoir. Whenever we do a field development, we build a geological model. These realistic geological models are required as input to reservoir simulator programs. Then we build one or more reservoir models and do extensive simulation to decide how to service the pipe lines, how to position the wells etcetera. After this step then we go into the production. At this stage, instead of using our reservoir models as a reference to influence our control decisions, we depend on spread sheet engineering and use creaming curves to make these decisions. These control inputs would then have to be manually fed in. We certainly do some surveillance, but it is based on some very simple models. After about five years into production, when we realize that our production does not really match what we predicted the first time, we would have to do a field re-development. Because of this, a new geological model is needed and we would also have to rebuild the reservoir model. Reservoir models are thus in fact “out of the loop” and hence the name “Open-loop Reservoir Management”.

Wouldn't it be much better and profitable if we could keep using our reservoir simulation models, by keeping them “ever-green” in order to optimize recovery?

Closed-loop reservoir management is based on the hypothesis that recovery can be significantly increased by changing reservoir from a batch-type use of reservoir simulation models to a near-continuous model-based control activity [2]. The key elements of this hypothesis are to perform:

- Optimization under physical constraints and geological uncertainties.
- Data assimilation aimed at continuous updating of the system models.

These two elements are in fact part of a broader theme under the concepts of system and control theory. The closed loop block diagram of optimal reservoir management as depicted in Figure 1-2, would not be different from any other closed-loop system encountered in most of the feedback control systems [3]. There have been several attempts to redraw the block diagram of Figure 1-2 to a more suitable system, which can be realized in the real-time [2] [4] [5] [6].

The top block in the figure represents the real world with the reservoir, the wells, and the facilities. To this block, there would be some kind of an input and some kind of an output. The inputs could be the rates at which water is injected through a well (for the purpose for water flooding) and the outputs could be the oil or water production. We simulate the real world with models of different kinds- the geological model, the reservoir models, the well models etcetera. Typically we use multiple models because the real world is uncertain. Once you have those models, some sort of optimization is required to complete the loop. At a high conceptual level, this can be field development and planning, and at a lower conceptual level it can be actually changing the injection and production rates of wells, optimizing gas lift rates etcetera. We also know that these models cannot correctly represent reality so prediction of the reservoir output for different inputs would be necessary. In this case, a comparison of the real output and some kind of history matching is used to update or correct the models.

For measuring outputs at the high conceptual level we can think about interpreting 4-D seismic data coming from geo-sensors, whereas in the lower conceptual

level we could get measurements by having extra sensors like in a production test. In this case we would be measuring the phase rates coming out of a single well.

This systematic updating of the model by comparing the predicted outputs with the actual outputs is what we call “Closed-Loop Reservoir Management”. The main issues when trying to perform a systematic update in the reservoir setting which hinder its direct applicability to real-time implementations are the large-scale nature of the reservoir models (state and parameters spaces) and the number of realizations of such uncertain parameters that need to be generated to completely describe the stochastic nature of these parameters [7] [8].

When we can look at this from a geosciences perspective, the geological model is at the core whereas when we think of reservoir modeling or become more focused on production, the flow model is at the core. In both cases we can combine optimization with data assimilation. Data assimilation involves using data from the well producing the oil to adapt the current reservoir model with the dynamics happening in the subsurface and trying to optimize production.

Several of these initiatives like i-fields and e-fields are focused on short term production optimization whereas one in reality would like to focus on a long term reservoir engineering perspective as well. In the hypothetical case we would like to have a single model, correctly representing the true world. Though it is unlikely, let us assume that we have it. Then the next question would be to what extent could we use the same model to optimize production. In order to carry out the concept of closed loop control over the lifetime of a reservoir, we would need to bring up a system where the

measurements can play a significant role in updating the reservoir model and would also need to come up with an optimization strategy that can work hand in hand with this continuously updated model [2] [9].

There are many ways to do optimization. In this thesis, optimal control theory is our choice. Optimal control theory was developed to control the trajectories of rockets by the Russians and the Americans in the 60s, but in reservoir engineering we use it to do history matching and flooding optimization. One of the key aspects is that we can deal with a lot of parameters. It is a gradient based technique that would give us a local optimum. This can be physically imagined as when we are trying to climb a hill and know that we have reached the top of the hill but we do not know whether we reached higher than the other hills which may be higher. We can optimize for the net present value or the ultimate oil recovery, or any other financial measure that we can compute from our reservoir model. We can manipulate several controls, the injection or production rates, and the pressure or valve openings. There may be hundreds or thousands of control variables and 10^4 to 10^6 state-space variables. Gradients are obtained by very efficient numerical techniques, and importantly it does result in a dynamic control. This would mean to dynamically change the inputs (the rates, the pressures etcetera) over time, - over the life of the reservoir. Optimization in our framework will be dealt with in Section 3.

Open Loop Reservoir Management

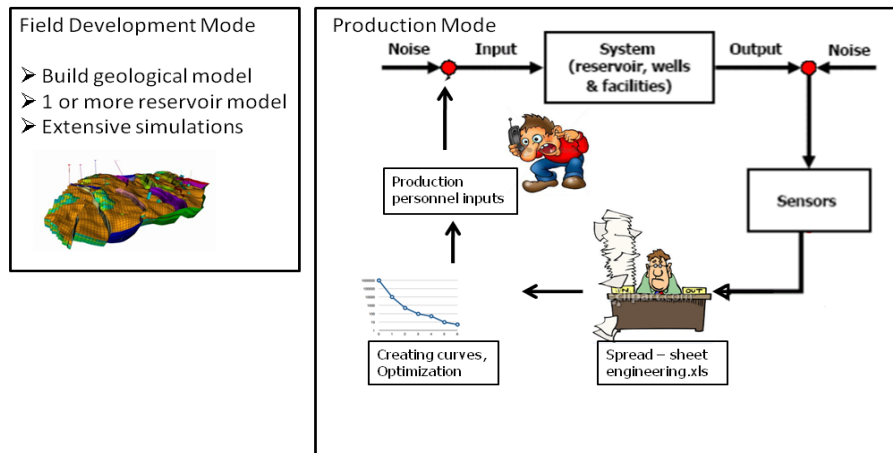


Figure 1-1 Block Diagram for Open-Loop Reservoir Management (adapted from [5])

Closed Loop Reservoir Management

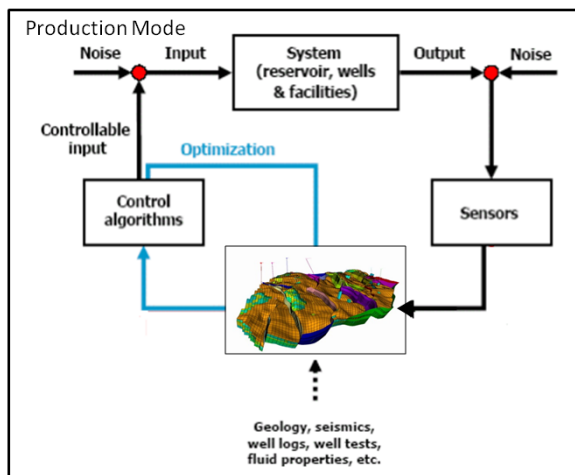


Figure 1-2 Block Diagram for Closed-loop Reservoir Management (adapted from [5])

Production optimization in the reservoir management context has been achieved by means of gradient-based methods or surrogate-based methods applied to a model assumed to be fixed in time and with no real-time adjustments for production data mismatch between the underlying models and production data.

Although this can lead to good results in practice, open loop optimization suffers from not having model corrections and change of scenarios embedded into the framework. On the other hand, in the closed-loop framework, model updating and optimization go hand in hand with the actual production data from the field. A well known technique in closed-loop optimization is called model predictive control (MPC). Based on the success of model-based optimization to the process industry, we aim to use MPC schemes to increase the potential for greater oil recovery, and therefore, enhanced reservoir management and profitability. MPC offers a robust control implementation together with constraint handling capabilities.

1.3 Problems with Large-Scale Systems and Model Order Reduction

As discussed above, reservoir models are typically very large dynamical systems. They are usually in the order of $\mathcal{O}(10^5 - 10^6)$ state variables. In order to use these reservoirs in a closed-loop control framework which would function in a real time sense, we would need to remarkably reduce the size of the model. This model reduction has been a field of interest within the mathematical and mechanical engineering community for a very long time, and it is quite relevant to the petroleum industry. The size and complexity of the underlying system with which our reservoir simulators run has always

raised a serious challenge for the application of systems and control. In this case, one can approximate the input-output behavior of such models in a process called model order reduction [10] [11] [12] [13].

Before I begin going into the details of the various type of model order reduction methods, let me give a brief about the underlying porous media flow equation that drive our large scale reservoir simulators. A detailed formulation is provided in Section 2 of the thesis.

In a mathematical framework, the model and controller reduction may be posed as follows:

One can show that, the porous media flow equations can be written as

$$\nabla \cdot \left[-\frac{\rho_i k_{ri}}{\mu_i} \mathbf{K} (\nabla p_i - \rho_i g \nabla h) \right] + \frac{\partial(\rho_i \phi S_i)}{\partial t} - \rho_i q_i = 0, \quad (1.1)$$

where (∇) is the gradient operator, \mathbf{K} is the permeability tensor, μ fluid viscosity, k_{ri} is the relative permeability of each phase (which is a function of S_w), p_i pressure of each phase, g is the acceleration of gravity and finally h is the depth of the reservoir, ρ is the fluid density, \mathbf{v} is the fluid superficial velocity, t is time, $(\nabla \cdot)$ denotes the divergence operator, ϕ is the porosity, S_i is the fluid saturation of each phase, q_i is flow rate per unit volume and finally $\{o, w\}$ represents the oil and water phases, respectively.

After discretization in space, each grid block is related to two states of the reservoir, that is, oil pressures and water saturations. Vectorizing the states of the system and denoting $\mathbf{X} = [p_o^1 \cdots p_o^N \ S_w^1 \cdots S_w^N]^T$, and similarly for the sources terms,

$\mathbf{Q} = [q_o^1 \ q_w^1 \ \dots \ q_o^N \ q_w^N]^T$, one can show that, the porous media flow equations Eq. 1.1 can be written in matrix form as

$$\mathbf{V}(\mathbf{X})\dot{\mathbf{X}} + T(\mathbf{X})\mathbf{X} = \mathbf{F}(\mathbf{X})\mathbf{Q}, \quad (1.2)$$

The interested reader can refer [4] and [5] for a detailed description of this equation. Here, each row of the matrix corresponds to the flow equation across each grid block in the reservoir. This equation can be seen as the input-output description of the underlying dynamical system [3] [14]. In this case, $\mathbf{V}(\mathbf{X})$ is the accumulation matrix, which contains ϕ , c_r , c_o and c_w , $\mathbf{T}(\mathbf{X})$ is the transmissibility matrix, containing the permeabilities and viscosity parameters, and $\mathbf{F}(\mathbf{X})$ is a selection matrix representing flow rates or bottom-hole pressure measurements. The above equation, in turn, can be recast in a generalized nonlinear state-space form and linearized through an operating point, yielding, the linear time-invariant continuous-time state-space formulation as

$$\begin{cases} \mathbf{g}(\mathbf{u}, \mathbf{x}, \dot{\mathbf{x}}, \boldsymbol{\theta}, t, \Pi) = \mathbf{0} \\ \mathbf{y}(t) = \mathbf{h}(\mathbf{u}, \mathbf{x}, \dot{\mathbf{x}}, \boldsymbol{\theta}, t, \Pi) \end{cases} \Rightarrow \begin{cases} \dot{\mathbf{x}}(t) = \mathbf{A}(\Pi)\mathbf{x}(t) + \mathbf{B}(\Pi)\mathbf{u}(t) \\ \mathbf{y}(t) = \mathbf{C}(\Pi)\mathbf{x}(t) + \mathbf{D}(\Pi)\mathbf{u}(t) \end{cases} . \quad (1.3)$$

One can note that in both cases, linear and nonlinear, a function dependency to Π was added to the equations, where Π is a vector of uncertain parameters of the system, for instance $\Pi = [K_1 \ \dots \ K_N, \phi_1 \ \dots \ \phi_N]^T$. As can be seen, the dimensions of the state-space \mathbf{X} and the parameter space Π are dependent upon the number of grid cells of the underlying PDE discretization. Therefore, large-scale models are obtained if accurate discretizations are sought after, requiring fine grid computations.

Given a dynamical system Σ , modeled as a non-linear differential equation, or in a special case, linear time-invariant dynamical system (LTI), one seeks a reduced order approximation to Eq. 1.3, such that:

- the dimension of the reduced order model is $r \ll n$;
- the behavior of the reduced order model approximates the original with certain accuracy, i.e., there is a small error bound on $\mathbf{y}(t) - \mathbf{y}_r(t)$;
- the model reduction procedure is computationally stable and efficient, and the reduced order model is achieved by means of projection, $\mathbf{\Pi} = \mathbf{VZ}^T$, where $\mathbf{V}, \mathbf{Z} \in \mathbb{R}^{n \times r}$ with $\mathbf{Z}^T \mathbf{V} = \mathbf{I}_r$, as in the following equations:

$$\Sigma_r : \begin{cases} \dot{\mathbf{x}}_r(t) = \mathbf{Z}^T \mathbf{F}(\mathbf{Vx}_r(t), \mathbf{u}(t), t) \\ \mathbf{y}_r(t) = \mathbf{Z}^T \mathbf{H}(\mathbf{Vx}_r(t), \mathbf{u}(t), t) \end{cases} \quad \text{or} \quad \Sigma_r : \begin{cases} \dot{\mathbf{x}}_r(t) = \mathbf{Z}^T \mathbf{A} \mathbf{Vx}_r(t) + \mathbf{Z}^T \mathbf{B} \mathbf{u}(t) \\ \mathbf{y}_r(t) = \mathbf{C} \mathbf{Vx}_r(t) + \mathbf{D}_r \mathbf{u}(t) \end{cases}$$

If the model equations are known explicitly, we can apply a model order reduction by projection as shown in Eq. 1.4. This is also called as a projection-based model order reduction which is a mathematically sound and efficient way of representing the model, as one approximates the state space variables x by a linear combination of basis vectors x_r as shown below.

$$x_n \approx \sum_{i=1}^r V_i x_{r_i} \quad (1.4)$$

$$[x_n] \approx [V][x_r]$$

Here, x is the actual state which is of dimension n which is a very large number, x_r is the reduced state which is of dimension $r \ll n$. By properly selecting V , one can deal with different types of dynamical systems. In order to determine the feasibility of the

application of various model reduction methods for designing low-order models and, in turn controllers, a study must be performed first at the reservoir model level, i.e., reservoir model reduction.

Several ways of obtaining reduced-order models were proposed in the literature [4] [14]. In a broad sense, they can be divided into two main categories: model reduction for simulation and model reduction for control purposes. In the latter case, one should recognize the importance of the addition of the controller into the process. In this manner, the problem of controller reduction (closed-loop) is different from the problem of model reduction (open-loop) given that the ultimate goal is to accurately approximate the closed-loop performance of the dynamical system.

In general, the problem of reducing the order of a large-scale model is known as the approximation of dynamical systems [14]. Basically one can view the approximation methodology simply as a surrogate model, as in the case of “black box” approaches, or one can intrusively modify the equation, as in the “white-box” approaches (see Figure 1-3).

Approximation Methods

SVD Methods	Krylov Subspaces	Nodal Truncation	Meta-modeling
<p>Linear Systems</p> <ul style="list-style-type: none"> Balanced Truncation Hankel Norm Approx. <p>Nonlinear Systems</p> <ul style="list-style-type: none"> POD Methods Empirical Gramian Empirical Interpolation TPWL 	<ul style="list-style-type: none"> Arnoldi Lanczos Rational Krylov Approximate Balancing 	<ul style="list-style-type: none"> FEM – upscaling Multiscale Modal Trunc. Ritz Reduction Guyan Reduction Dynamic Cond. AMLS 	<ul style="list-style-type: none"> Surrogates Proxy Neural Nets Subspace Identification

Figure 1-3 Model Order Reduction Techniques (adapted from [14])

Based on the type of Model Order Reduction (MOR), we come up with one of the reduction methods as shown in Figure1-3 which is by no means a comprehensive table with all possible methods.

In the Section that follows, we will explain the differences between the white box and black box approach and briefly describe the following methods for model reduction: Balanced truncation, Proper Orthogonal Decomposition and Subspace Identification.

1.3.1 White Box

If the model equations are known, one can apply model reduction by projection by the white box approach [14]. In this approach, basically three families of model reduction may be used. This can be classified into SVD method; Krylov based subspaces

or moment matching methods and Nodal Truncation. All the methods in the white-box approach would entail the modification of the equations of the dynamical system. For this, one needs to have at hand, the source code of the reservoir simulator, and perform modifications to it. Several techniques have been developed in both the linear dynamical system framework, namely, the Balanced Truncation, Hankel Norm Approximation, Moment Matching by Krylov Techniques, and, in the nonlinear setting, namely the use of the Proper Orthogonal Decomposition (POD) and its variants [14].

Roughly speaking, the SVD family relies on dense matrix factorizations and preserves important theoretical properties of the original system, like stability, together with a measure of the approximation error. The Krylov methods on one hand rely only on matrix vector multiplications, yielding numerically efficient algorithms for large-scale applications, but on the other hand they lack good theoretical properties. A combination of the best features of both families is also possible in an SVD-Krylov framework through the use of iterative methods [14]. As far as Nodal Truncation methods as concerned, they find their applicability in the discretization of partial differential equations, where one finds methods such as the finite element methods (FEM). In this case, we can pose model order reduction in a projection framework by using what is called the nodal truncation methods.

1.3.1.1 Balanced Truncation

One of the best model reduction techniques applied to linear dynamical systems is known as balanced truncation. It has been used extensively by the control and

structural dynamics communities for obtaining reduced order models for control purposes [14]. The main feature of this method is the retention of stability and a priori computable error bounds. Notably, as will be seen later, balanced truncation has been extended to the nonlinear case by means of proper orthogonal decompositions (PODs) [10] [12] [14].

Basically, the method relies on the computation of a similar transformation to simultaneously diagonalize two matrices, the so-called controllability and observability gramians of the system, obtained by the solution of two Lyapunov equations, yielding the projection matrices to be used in the reduction process.

It has been known in the control engineering community [14] [15] that the controllability and observability gramians are related to the energy needed to steer a system from an initial condition $\mathbf{x}_0=\mathbf{0}$ to a final state \mathbf{x} , and the energy required to observe the output of the system with initial condition \mathbf{x} and no excitation function, respectively. So, simultaneously diagonalizing the gramians gives good insight into the states that require large amounts of energy to be controlled or that yield small amounts of observation energy, and, therefore may be eliminated without a significant impact on the system response.

Given the dynamical system as in Eq. 1.2, one can define, respectively, the controllability and observability gramians as

$$\mathbf{A}\mathbf{P}+\mathbf{P}\mathbf{A}^*+\mathbf{B}\mathbf{B}^*=\mathbf{0}, \quad \mathbf{A}^*\mathbf{Q}+\mathbf{Q}\mathbf{A}+\mathbf{C}^*\mathbf{C}=\mathbf{0}$$

A similar transformation, \mathbf{T} , can be found in Eq. 1.2 to simultaneously diagonalize the gramians as

$$\tilde{\mathbf{P}} = \mathbf{T}\mathbf{P}\mathbf{T}^* = \tilde{\mathbf{Q}} = \mathbf{T}^{-*}\mathbf{Q}\mathbf{T}^{-1} = \mathbf{\Sigma} = \text{diag}(\sigma_1\mathbf{I}_{m_1}, \dots, \sigma_q\mathbf{I}_{m_q})$$

In this case, the diagonal elements of $\mathbf{\Sigma}$ are called the Hankel singular values of the system. The reduced model can be obtained by means of a projection, based on the partition of $\mathbf{\Sigma}$, where $\mathbf{\Sigma}_2$ represents the small singular values of the system.

$$\mathbf{G}(s) = \left[\begin{array}{c|c} \mathbf{TAT}^{-1} & \mathbf{TB} \\ \hline \mathbf{CT}^{-1} & \mathbf{D} \end{array} \right] = \left[\begin{array}{cc|c} \mathbf{A}_{11} & \mathbf{A}_{12} & \mathbf{B}_1 \\ \mathbf{A}_{21} & \mathbf{A}_{22} & \mathbf{B}_2 \\ \hline \mathbf{C}_1 & \mathbf{C}_2 & \mathbf{D} \end{array} \right]$$

$$\mathbf{G}_r(s) = \left[\begin{array}{c|c} \mathbf{A}_{11} & \mathbf{B}_1 \\ \hline \mathbf{C}_1 & \mathbf{D} \end{array} \right] \text{ and } \mathbf{\Sigma} = \begin{bmatrix} \mathbf{\Sigma}_1 & \mathbf{0} \\ \mathbf{0} & \mathbf{\Sigma}_2 \end{bmatrix} \quad (1.5)$$

It can be shown [10] [14] [15] that there exists *a priori* computable error bound for the above approximation.

1.3.1.2 POD

Proper Orthogonal Decomposition (POD), also known as principal component analysis, or the Karhunen-Loève, is one of the most prominent model reduction techniques for large-scale nonlinear models. Proper orthogonal decomposition has been successfully used in several fields, including the computational fluid dynamics community, signal analysis and pattern recognition, and in control theory [10] [14]. Recently POD and its variants have been applied somewhat successfully to the reservoir simulation arena [2] [10] [11] [12].

This method essentially provides an orthonormal basis for representing the given data in a certain least squares optimal sense, and truncation of the optimal basis provides

a way to find optimal lower dimensional approximations of the given data. One seeks a projection, \mathbf{P}_r , of fixed rank r , such that the following cost is minimized:

$$\int_0^T \|\mathbf{x}(t) - \mathbf{P}_r \mathbf{x}(t)\|^2 dt$$

It can be shown that a necessary condition for Eq. 1.5 to hold is that \mathbf{P}_r is an

eigenfunction of the kernel $\mathbf{R} = \int_0^T \mathbf{x}(t) \mathbf{x}^*(t)$, defined by, $\mathbf{R} \varphi_k = \lambda_k \varphi_k$. The main result of POD approximation is that the optimal subspace of dimension r is spanned by a truncation of the eigenvectors of the kernel as

$$\mathbf{P}_r = \sum_{k=1}^r \varphi_k \varphi_k^*$$

Since the computation of the kernel is a difficult task to be performed in the nonlinear case, the method of snapshots was introduced as a way of determining the eigenfunctions without explicitly computing the kernel R . In this case, one defines the correlation matrix as

$$\mathbf{R} = \frac{1}{m} \sum_{j=1}^m \mathbf{x}(t_j) \mathbf{x}^*(t_j)$$

where $\mathbf{x}(t_j)$ is the instantaneous system state or snapshot at time t_j . Since \mathbf{R} is symmetric and positive definite, one can compute its basis, \mathbf{P}_r , by means of the thin singular value decomposition (SVD) of the kernel as $\mathbf{R} = \mathbf{P}_r \mathbf{S}_r \mathbf{V}_r^*$. Model reduction is then accomplished by projection into the nonlinear equations.

The keen reader can realize the close connections between POD's and the balanced truncation method [14]. In this sense, if one experiments with the linear system given by Eq. 1.3, by choosing the input functions as the impulse $\delta(t)$, one can recover the controllability gramian as the kernel of the nonlinear system. This yields the so-called Balanced POD by means of empirical gramians.

1.3.2 Black Box

When one works with mainly commercial-out-of-the-shelf reservoir simulators, one has only access to input and output data. In this case, one can work with the black-box methods in which the reduced order model is obtained by looking at the relation between the inputs and outputs of the system. There are many ways to deal with input/output data. One can generate artificial intelligence systems, such as the neural nets, proxy models, etc, to train the production history into a computer code, so that it can predict future outcomes. Of the various meta-modeling or black box approaches as shown in Figure 1.3, the one on which I will be focusing in this thesis will be subspace identification.

1.3.2.1 Subspace Identification

In the early 90's, subspace identification techniques [16] [17] were originated as a generalization of the classical realization theory developed in the systems framework, with the addition of concepts from numerical linear algebra and geometry. Essentially,

subspace identification is a "black-box" approach that extracts a linear model from the sequence of inputs and outputs generated from a simulator [16] [17] based on the idea of controllability and observability and balanced realizations as explained before. The identification process always consists in two steps: (1) weighted projection of the row space of a well-defined matrix from input/output data, the so-called data Hankel matrix, and in turn the estimation of the state sequence; and (2) the actual computation of the system matrices through a least-square approach using the above estimated states.

It can be shown that the state-space basis of the subspace identified models can coincide with a frequency weighted balanced basis for appropriate weights. This is a nice result, since one can compute reduced-order models from input/output data by looking at the decay of the frequency weighted Hankel singular values.

However in this thesis, as we would be using an in-house simulator to perform the optimization, we would be considering the black-box approach namely the subspace identification methods. In this case, we will use the input/output behavior of the dynamical system (from the commercial reservoir simulator that we intend to use) to generate the **A**, **B**, **C**, **D** state space matrices that would be used in our control framework. Further details about System Identification would be provided in Section 4.

1.4 Objectives of the Proposed Research

In this thesis we would primarily be focusing on improving the secondary-recovery of a reservoir using water flooding. As the title implies we would be focusing on the control concept called model predictive control and on system identification to

carry out our optimization process for water flooding. A number in injection wells will be drilled to inject water and thus maintain a somewhat steady reservoir pressure and thus sweep the reservoir. A number of wells would be required to be drilled in various parts of the reservoir to effectively retrieve oil. The problem lies in the fact that as time progresses, the water injected would flow favorably toward the channelized structure of the porous media, and then we would start producing uneconomical quantities of water.

The use of smart control over injection and production wells would expand the possibilities to control and manipulate the fluid paths through the reservoir. Thus we could somewhat manipulate the progression of oil/water front in such a way so as to result in the maximum possible ultimate oil recovery.

Some of the challenges that the industry currently faces as pointed out in the Digital Energy Conference -2011 [18] with regard to closed-loop reservoir management are:

- What is the optimal frequency for the updating of reservoir models and production strategies?
- How can we best combine long-term reservoir management with short-term production optimization?
- What are the observable and controllable variables in our reservoir models and which parameters can be identified from data?
- What is the optimal level of detail (both in space and time) for control-relevant reservoir models?

- What are the most important decisions, and how can we focus our measurement strategy and modeling efforts to support those?
- What is the scope to apply closed-loop reservoir management in secondary and tertiary recovery?
- What can we learn from other disciplines such as industrial process control, meteorology and oceanography?
- Can we use them to influence the flow in the subsurface rather than just to automate the push of a button?

Most of these issues will be dealt with on the thesis. In this thesis, I seek to explain how real-time optimal control can be to reservoir management by studying the reservoir production from two models in particular. Based on the observations from the various test that were conducted on the reservoirs, we suggest the use of MPC schemes to increase the potential for greater oil recovery. This would obviously ensure enhanced reservoir management and profitability.

At first, an overview of the dynamics of a two-phase reservoir is dealt with by referring to the basic equations for flow in porous media. Then a mathematical treatment of subspace identification and MPC as applied to reservoir simulation will be presented. Then linear MPC performance would be studied on two specific reservoir models after generating low-order reservoir models using subspace identification methods. Lastly, the highly nonlinear behavior of the models will be highlighted and the use of nonlinear MPC will be suggested. All the comparisons are provided from a set of realistic simulations using the commercial reservoir simulator called Eclipse®.

2. RESERVOIR SIMULATION AND PRODUCTION OPTIMIZATION

2.1 Introduction to Porous Media Flow

The electronic explosion that we can witness in our generation has transformed reservoir simulation from an esoteric tool to a practical toolbox of immense importance. With the explicit use of this tool, today's engineering community has had the opportunity to better understand not only the intricate details and dynamics of fluid flow in the reservoir, but also the characteristics of fluid flow patterns in the immediate vicinity of perforations, wellbore, pressure and saturation dynamics of horizontal, slanted, vertical and multilateral wells; in addition to considerations of complexities in reservoir characterizations.

2.2 Partial Differential Equations

Reservoir simulation has always been one of the main components in reservoir management. Great effort has been devoted to constructing high-order reservoir models for improved oil recovery [19] [20]. In general, the governing equations of multi-phase flow in porous media are given by a set of partial differential equations that represent conservation of mass, momentum and energy together with equations of state which describe the fluid property as a function of pressure and temperature.

As discussed in [19] [20], several simplifications can be taken into account such as neglected inertial effects, flow being isothermal and the use of the empirical Darcy's

law. Hence, one can assume the "Black-oil" formulation, where there are two components (oil-water) and there are two phases of the hydrocarbon substance (oil and gas) present in the reservoir. In this paper, we will assume no gas in the reservoir. The mass balance equation for each phase is given by

$$\nabla \cdot (\rho_i \mathbf{v}_i) + \frac{\partial(\rho_i \phi S_i)}{\partial t} - \rho_i q_i = 0, \quad i \in \{o, w\}, \quad (2.1)$$

where ρ is the fluid density, \mathbf{v} is the fluid superficial velocity, t is time, $(\nabla \cdot)$ denotes the divergence operator, ϕ is the porosity, S_i is the fluid saturation of each phase, q_i is flow rate per unit volume and finally $\{o, w\}$ represents the oil and water phases, respectively. Using the empirical Darcy's law, one can write

$$\mathbf{v}_i = -\frac{k_{ri}}{\mu_i} \mathbf{K} (\nabla p_i - \rho_i g \nabla h), \quad (2.2)$$

where (∇) is the gradient operator, \mathbf{K} is the permeability tensor, μ fluid viscosity, k_{ri} is the relative permeability of each phase (which is a function of S_w), p_i pressure of each phase, g is the acceleration of gravity and finally h is the depth of the reservoir. Plugging Eq. 2.1 into Eq. 2.2, one writes

$$\nabla \cdot \left[-\frac{\rho_i k_{ri}}{\mu_i} \mathbf{K} (\nabla p_i - \rho_i g \nabla h) \right] + \frac{\partial(\rho_i \phi S_i)}{\partial t} - \rho_i q_i = 0. \quad (2.3)$$

With four unknowns p_w, p_o, S_w, S_o , four equations are required to complete the system description and solve Eq. 2.3. The two additional equations are given by a closure equation which states that the sum of all fractional saturations must always be equal to one, and the oil-water capillary pressure equation, which gives a relation between phase pressures, as a function of water saturation. They are respectively;

$$S_w + S_o = 1, \quad (2.4)$$

$$p_o - p_w = p_c(S_w) \quad (2.5)$$

All the equations Eq.2.1, Eq.2.2, Eq.2.3, Eq.2.4 and Eq.2.5 can be rearranged in such a way that the two-phase equations are formulated in terms of two state variables - p_o , the oil pressure, and S_w , the water saturation. In order to do that one can apply the chain rule differentiation and the definitions of oil, water and rock compressibilities as

$$c_i = \left. \frac{1}{\rho_i} \frac{\partial \rho_i}{\partial p_i} \right|_{T_R}, \quad i \in \{o, w\}; \quad c_r = \frac{1}{\phi} \frac{\partial \phi}{\partial p_o},$$

yielding

$$\begin{aligned} -\nabla \cdot \left[\frac{\rho_w k_{rw}}{\mu_w} \mathbf{K} \left\{ \left(\nabla p_o - \frac{\partial p_c}{\partial S_w} \nabla S_w \right) - \rho_w g \nabla h \right\} \right] + \rho_w \phi \left[S_w (c_w + c_r) \frac{\partial p_o}{\partial t} + \frac{\partial S_w}{\partial t} \right] \\ - \rho_w q_w = 0, \\ -\nabla \cdot \left[\frac{\rho_o k_{ro}}{\mu_o} \mathbf{K} \{ \nabla p_o - \rho_o g \nabla h \} \right] + \rho_o \phi \left[(1 - S_w) (c_o + c_r) \frac{\partial p_o}{\partial t} + \frac{\partial S_w}{\partial t} \right] - \rho_o q_o = 0, \end{aligned} \quad (2.6)$$

As can be seen from the above equations, multiphase flow through porous media is given by a set of weakly-nonlinear parabolic PDE's that represents the dynamics of the rate of change of pressure (diffusion) coupled with a set of strongly-nonlinear parabolic-hyperbolic PDE's which describe the dynamics of the rate of change in phase saturations and component concentrations (diffusion-convection). The equations can be discretized in space yielding a set of ordinary differential equations. Most of the numerical reservoir simulators apply a spatial discretization scheme based on finite

differences or finite volume formulations, using an upstream weighting in the convection dominant terms.

These multiphase porous media flow equation when evaluated at every grid block for a 2 dimensional reservoir that has a two-phase flow (Oil and Water) would take the following form when the liquids are assumed to be slightly compressible [1].

$$S_{i,j}^n (P_{i,j-1}^{n+1} - P_{i,j}^{n+1}) + W_{i,j}^n (P_{i-1,j}^{n+1} - P_{i,j}^{n+1}) + E_{i,j}^n (P_{i+1,j}^{n+1} - P_{i,j}^{n+1}) + N_{i,j}^n (P_{i,j+1}^{n+1} - P_{i,j}^{n+1}) = \frac{B^{n+1}}{\Delta t} (P_{i,j}^{n+1} - P_{i,j}^n) - q_{lsc,i,j}^{n+1} \quad (2.7)$$

Here, S, W, E, and N account for the transmissibility through the south, west, east and north grid boundaries respectively for each grid cell in the reservoir based on a five point stencil as shown in Figure 2-1.

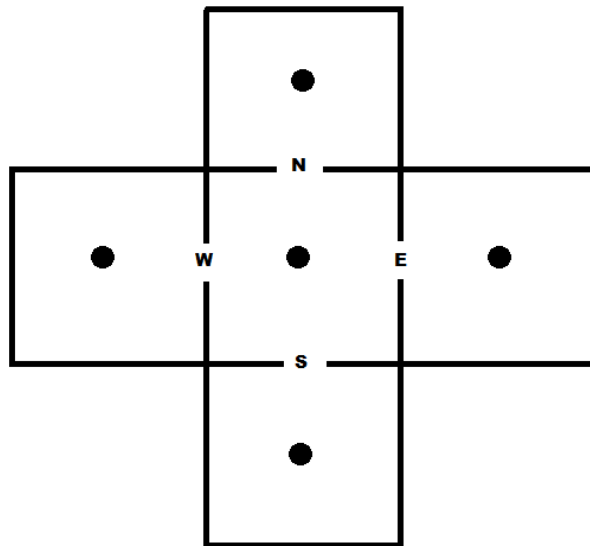


Figure 2-1 Grid Cell Transmissibility

The transmissibility equations are given by

$$S_{i,j} = T_{ly_{i,j-1/2}} = \left(\beta_c \frac{A_y k_y}{\mu_l B_l \Delta y} \right)_{i,j-1/2}$$

$$W_{i,j} = T_{lx_{i,j-1/2}} = \left(\beta_c \frac{A_x k_x}{\mu_l B_l \Delta x} \right)_{i-1/2,j}$$

$$E_{i,j} = T_{lx_{i+1/2,j}} = \left(\beta_c \frac{A_x k_x}{\mu_l B_l \Delta x} \right)_{i+1/2,j}$$

$$N_{i,j} = T_{ly_{i,j+1/2}} = \left(\beta_c \frac{A_y k_y}{\mu_l B_l \Delta y} \right)_{i,j+1/2}$$

Eq. 2.7 can be rewritten using implicit formulation (which will be described in the end of this Section) as

$$S_{i,j}^n P_{i,j-1}^{n+1} + W_{i,j}^n P_{i-1,j}^{n+1} + E_{i,j}^n P_{i+1,j}^{n+1} + N_{i,j}^n P_{i,j+1}^{n+1} + C_{i,j}^n P_{i,j}^{n+1} = \frac{B^{n+1}}{\Delta t} (P_{i,j}^{n+1} - P_{i,j}^n) - q_{lsc_{i,j}}^{n+1} \quad (2.8)$$

The transmissibility term C and the flow rate term $q_{lsc_{i,j}}^{n+1}$ in the above equation is computed as follows. For grid blocks without wells and for grid blocks hosting rate specified wells,

$$C_{i,j} = -[S_{i,j} + W_{i,j} + E_{i,j} + N_{i,j}]$$

$$q_{lsc_{i,j}}^{n+1} = q_{lsc_{i,j}}^{n+1}$$

For grid blocks hosting pressure specified wells,

$$C_{i,j} = -[S_{i,j} + W_{i,j} + E_{i,j} + N_{i,j} + J_{i,j}]$$

$$q_{lsc_{i,j}}^{n+1} = -J_{i,j} p_{wf}$$

The symbol B in the two-phase flow equation “” and the matrix \mathbf{B} in the matrix form of the two-phase flow equation “” accounts for the accumulation terms. The matrix \mathbf{B} takes the form;

$$\mathbf{B} = \begin{bmatrix} [\mathbf{e}_{op}] & [\mathbf{e}_{ow}] \\ [\mathbf{e}_{wp}] & [\mathbf{e}_{ww}] \end{bmatrix};$$

where

$$\mathbf{e}_{op} = \begin{bmatrix} e_{op_1} & & & & \\ & e_{op_2} & & & \\ & & \cdot & & \\ & & & \cdot & \\ & & & & \cdot & \\ & & & & & e_{op_N} \end{bmatrix}$$

$$\mathbf{e}_{ow} = \begin{bmatrix} e_{ow_1} & & & & \\ & e_{ow_2} & & & \\ & & \cdot & & \\ & & & \cdot & \\ & & & & \cdot & \\ & & & & & e_{ow_N} \end{bmatrix}$$

$$\mathbf{e}_{wp} = \begin{bmatrix} e_{wp_1} & & & & \\ & e_{wp_2} & & & \\ & & \cdot & & \\ & & & \cdot & \\ & & & & \cdot & \\ & & & & & e_{wp_N} \end{bmatrix}$$

$$\mathbf{e}_{ww} = \begin{bmatrix} e_{ww_1} & & & & \\ & e_{ww_2} & & & \\ & & \cdot & & \\ & & & \cdot & \\ & & & & \cdot & \\ & & & & & e_{ww_N} \end{bmatrix}$$

The subscript in each term here corresponds to the grid index of the cell for which the accumulation terms e_{op} , e_{ow} , e_{wp} and e_{ww} are computed. These accumulation terms are computed as per the following equations,

Rearranging the equation, we can derive its state space form as follows.

$$\mathbf{B} \frac{d\mathbf{x}}{dt} - \mathbf{T}\mathbf{x} = -\mathbf{Q}$$

$$\dot{\mathbf{x}} = (\mathbf{B}^{-1}\mathbf{T})\mathbf{x} - (\mathbf{B}^{-1}\mathbf{Q}) \quad (2.10)$$

where

$$\mathbf{Q} = \mathbf{W} \cdot \mathbf{u}$$

' \mathbf{W} ' is the selection matrix. Its size depends on the number of wells to be controlled and the total number of grids in the reservoir. ' \mathbf{u} ' is the input matrix for the wells. For instance, if we are dealing with a reservoir that has a total of 10 grid cells and have 5 wells that need to be controlled, the size of ' \mathbf{W} ' would be 20 x 10 and the size of ' \mathbf{u} ' would be 20 x 1. This is explained as follows.

The matrix \mathbf{W} is generally a very sparse matrix. The input wells can either be controlled by manipulating the flow rates (rate specified wells) or by manipulating the bottom hole pressures (pressure specified). In our formulation, if for instance well number one, four and five were rate specified, then the columns one, four and five in the selection matrix would have an entry (of value one) at the row corresponding to the grid index of its respective well. In a similar fashion if well number two and three were

pressure specified, the columns two and five in the well selection matrix would have an entry (of value corresponding to the productivity index of the well) at the row corresponding to the grid index of its respective well. This is illustrated in Table 1-1.

Table 1-1 Example to Illustrate State-Space Formulation

Well number	Well Type	Control Type	Grid Index	Well Productivity (Oil)	Well Productivity (Water)
1	Injection	Rate	6	J_{i1}^o	J_{i1}^w
2	Production	Pressure	3	J_{p2}^o	J_{p2}^w
3	Injection	Pressure	10	J_{i3}^o	J_{i3}^w
74	Production	Rate	4	J_{p4}^o	J_{p4}^w
5	Production	Rate	8	J_{p5}^o	J_{p5}^w

$$\mathbf{W}_o = \begin{bmatrix} 0 & 0 & 0 & 0 & 0 \\ 0 & 0 & 0 & 0 & 0 \\ 0 & J_{p2}^o & 0 & 0 & 0 \\ 0 & 0 & 0 & 1 & 0 \\ 0 & 0 & 0 & 0 & 0 \\ 1 & 0 & 0 & 0 & 0 \\ 0 & 0 & 0 & 0 & 0 \\ 0 & 0 & 0 & 0 & 1 \\ 0 & 0 & 0 & 0 & 0 \\ 0 & 0 & J_{i3}^o & 0 & 0 \end{bmatrix} ; \quad \mathbf{W}_w = \begin{bmatrix} 0 & 0 & 0 & 0 & 0 \\ 0 & 0 & 0 & 0 & 0 \\ 0 & J_{p2}^w & 0 & 0 & 0 \\ 0 & 0 & 0 & 1 & 0 \\ 0 & 0 & 0 & 0 & 0 \\ 1 & 0 & 0 & 0 & 0 \\ 0 & 0 & 0 & 0 & 0 \\ 0 & 0 & 0 & 0 & 1 \\ 0 & 0 & 0 & 0 & 0 \\ 0 & 0 & J_{i3}^w & 0 & 0 \end{bmatrix}$$

$$\mathbf{W} = \begin{bmatrix} \mathbf{W}_o & \mathbf{0} \\ \mathbf{0} & \mathbf{W}_w \end{bmatrix}$$

$$\mathbf{u}_o = \begin{bmatrix} \widetilde{\mathbf{q}}_o \\ \widetilde{\mathbf{p}}_o \end{bmatrix}; \quad \mathbf{u}_w = \begin{bmatrix} \widetilde{\mathbf{q}}_w \\ \widetilde{\mathbf{p}}_w \end{bmatrix}; \quad \mathbf{u} = \begin{bmatrix} \mathbf{u}_o \\ \mathbf{u}_w \end{bmatrix};$$

As mentioned above, the inputs can either be rate specified or pressure specified. Thus the size of the column vectors $\tilde{\mathbf{q}}$ and $\tilde{\mathbf{p}}$ depends on the number of rate specified and pressure specified wells respectively. For the example considered above we would thus have the column vector $\tilde{\mathbf{q}}$ of size 3 x 1 and the column vector $\tilde{\mathbf{p}}$ of size 2 x 1.

Eq. 2.10 can be written in the state-space form as

$$\dot{\mathbf{x}} = \mathbf{A} \mathbf{x} + \mathbf{B} \mathbf{u}$$

where \mathbf{A} and \mathbf{B} are two of the state space matrices. The remaining two matrices \mathbf{C} and \mathbf{D} required for the complete state space formulation comes from the measurement equations as described below.

An important point to be noted is that if the same well is used for both monitoring the outputs and manipulating the inputs, then if the inputs are specified, the measurements that would be made would be the bottom hole pressures and vice versa. For most cases, the same well would serve for both output measurements and input manipulation. For the example described above, we would have the measurement vector \mathbf{y} as follows;

$$\mathbf{y} = \begin{bmatrix} \bar{p} \\ \bar{q} \end{bmatrix}$$

in which the size of \bar{p} and \bar{q} depends on how many outputs we would like to measure. The calculation for the measurements can be made using the well productivity index formula. It is with these equations that we derive the state space matrices \mathbf{C} and \mathbf{D} .

The well productivity index formula at the wells for which would like to measure the outputs would take of the form shown below;

For rate specified wells, we would want to measure the bottom hole pressures given by

$$\bar{p} = p_{grid} \pm J_l^{-1} \tilde{q}_l \begin{cases} + \text{ for injection wells} \\ - \text{ for production wells} \\ l = \text{ oil or water} \end{cases} \quad (2.11)$$

For pressure specified wells, we would want to measure the rates given by

$$\bar{q}_l = \pm J_l (p_{grid} - \tilde{p}) \begin{cases} - \text{ for injection wells} \\ + \text{ for production wells} \\ l = \text{ oil or water} \end{cases} \quad (2.12)$$

The state space equation would be of the form

$$\mathbf{y} = \mathbf{C} \mathbf{p} + \mathbf{D} \mathbf{u}$$

where $\mathbf{y} = \begin{bmatrix} \bar{p} \\ \bar{q}_l \end{bmatrix}$

$$\mathbf{C} = \begin{bmatrix} \mathbf{C}_o & \mathbf{0} \\ \mathbf{C}_w & \mathbf{0} \end{bmatrix}$$

$$\mathbf{D} = \begin{bmatrix} \mathbf{D}_o & \mathbf{0} \\ \mathbf{0} & \mathbf{D}_w \end{bmatrix}$$

Suppose we wanted to measure the outputs at well number one, two and three for the case discussed above. Since well number one is a rate specified well, we would want to measure its bottom hole pressure. Similarly for the well number two, since it is a pressure specified well, we would want to measure the rates. The rates that we can measure for well two can be its oil production rate, water production rate or the liquid rate. Since we are considering a two phase flow, the liquid rate is assumed to be the sum of the oil and water production rates. For well number two let us measure its oil production. The well number three is also defined as a pressure specified well, and we would want to measure its rates. But this case is quite different from that of well number

two as we are dealing with an injection well. Since the only fluid we would be injecting is water, the water injection rate is the only quantity that can be measured at this well.

The state space matrices \mathbf{C} and \mathbf{D} would take the form;

$$\mathbf{C}_o = \begin{bmatrix} 0 & 0 & 0 & 0 & 0 & 1 & 0 & 0 & 0 & 0 \\ 0 & 0 & -J_{p2}^o & 0 & 0 & 0 & 0 & 0 & 0 & 0 \\ 0 & 0 & J_{i3}^o & 0 & 0 & 0 & 0 & 0 & 0 & 0 \end{bmatrix}$$

$$\mathbf{C}_w = \begin{bmatrix} 0 & 0 & 0 & 0 & 0 & 1 & 0 & 0 & 0 & 0 \\ 0 & 0 & -J_{p2}^w & 0 & 0 & 0 & 0 & 0 & 0 & 0 \\ 0 & 0 & J_{i3}^w & 0 & 0 & 0 & 0 & 0 & 0 & 0 \end{bmatrix}$$

$$\mathbf{D}_o = \begin{bmatrix} J_{i1}^{o-1} & 0 & 0 \\ 0 & -J_{p2}^o & 0 \\ 0 & 0 & J_{i3}^o \end{bmatrix}$$

$$\mathbf{D}_w = \begin{bmatrix} J_{i1}^{w-1} & 0 & 0 \\ 0 & -J_{p2}^w & 0 \\ 0 & 0 & J_{i3}^w \end{bmatrix}$$

In this manner Eq. 2.11 and Eq. 2.12 can in turn be recast in a generalized nonlinear state-space form and linearized through an operating point, yielding, the linear time-invariant state-space formulation

$$\dot{\mathbf{x}} = \mathbf{A} \mathbf{x} + \mathbf{B} \mathbf{u}$$

$$\mathbf{y} = \mathbf{C} \mathbf{p} + \mathbf{D} \mathbf{u}$$

for the porous media flow equations that govern a reservoir; where the matrices \mathbf{A} , \mathbf{B} , \mathbf{C} and \mathbf{D} denotes the states and controls Jacobians obtained in the linearization process, would fully define our system- the reservoir model at each time step.

2.4 Introduction to Reservoir Simulation – Solution Methods

Multiphase-flow simulation results in multiple finite-difference equations for each gridblock. We would have one equation for each component for each gridblock. The basic solution methods that are currently in use for solving the difference equations fall into three categories. These are the SS (Simultaneous Solution), the IMPES (Implicit Pressure Explicit Saturation) and the SEQ (Sequential Solution) method. Out of all these methods, the most powerful is the fully implicit method (also called Newton's method)- which falls in the Simultaneous Solutions category.

The Newton's Method has always been recognized to be the natural option to solve nonlinear system of equations. Though it has always remained quite powerful, its application to numerical reservoir simulation was not feasible in the beginnings due to limitations in computation power then. After a marked improvement in computer technology especially during the late 70's and early 80's, the application of this simultaneous solution method became a lot more practical within the industry. It covered a wide spectrum in its applicability; which includes the modeling of the coning process, compositional simulation, and other complex problems like multiphase flow in reservoir etc. Though it is computationally the most expensive solution method, a noticeable advantage in this method when compared to the others was in its retaining of stability characteristics independent of the time steps used for computation.

An alternate linearization method to this called IMPES was developed and used by the industry for various field studies. The storage and computer time requirements of IMPES are considerably less than those of Simultaneous Solution, making it the best

choice in reservoir simulation studies. The main problem with this method is its weak numerical stability especially in application to coning problems. Thus small time steps are required to maintain the stability while applying the IMPES solution method,.

The third method called the Sequential Solution method was developed with the objective to improve the stability of the IMPES method without solving for the oil pressure and saturations simultaneously. This is achieved by solving the equations for pressure implicitly in the first step and then solving for the saturation implicitly in the subsequent step. The first step of the Sequential Solution method is identical to the IMPES method as both perform an implicit pressure solution. The Sequential Solution method may be derived by the use of either the linear implicit-flow equations or the mass-conservation equations combined with the fractional-flow equations. For this case, since the oil pressure and saturations are solved independently, material balance will not be satisfied for all the phases present. A comprehensive study of these solutions methods including other alternate methods like Semi-Implicit, LSI, SI and adaptive Implicit Methods is provided in [1].

For our simulator, though we have coded with both Implicit and IMPES solution methods, we would primarily use the implicit solution method since we would have more freedom in testing with various time steps and not worry about any stability issues. Though this is the case, when the actual MPC code is implemented, we would build on a commercial simulator rather than on the reservoir simulator we developed.

3. INTRODUCTION TO MODEL PREDICTIVE CONTROL

Predictive control is an overarching term for a suite of control strategies mostly developed in the process industry during the 1970s. Since then, there has been a plethora of names denoting particular variants of predictive control. Examples of these are:

- Generalized Predictive Control (GPC)
- Dynamic Matrix Control (DMC)
- Extended Prediction Self-Adaptive Control (EPSAC)
- Predictive Functional Control (PFC)
- Sequential Open Loop Optimization (SOLO)
- Model Algorithmic Control (MAC)
- Quadratic Dynamic Matrix Control (QDMC)

and so on. A controller which is based upon one of these strategies would select control inputs by the online optimization of a predefined cost function at discrete time intervals. The generic names by which the whole area of predictive control is denoted including the ones mentioned above are Model Predictive Control, or MPC, and Model-Based Predictive Control, or MBPC.

MPC is well suited for multiple-input, multiple-output (MIMO) control. MPC allows for explicit handling of input, output, and state constraints (i.e. if a set of control inputs violate a constraint as predicted by the dynamic model, that set of inputs is discarded as a possible choice). In addition, MPC-based controllers can have a high level of flexibility in meeting general operational goals as the operating conditions change.

The concepts of MPC have already found attractive and powerful applications in measuring and controlling various large-scale systems in oceanography, meteorology and the process industry. Most of its interest is particularly attractive to closed-loop reservoir management from its ability to handle constraints, and from the natural way by which it can be applied to control multivariable systems like large-scale reservoir models without losing the intuitive aspect.

3.1 The Basic Formulation

Even before beginning to explain the formulation, it is important to get accustomed to some of the definitions and get an idea of the step by step algorithm in which MPC works. To illustrate the way the proposed MPC controller would work, a generic example is presented at first and later an explanation of how this algorithm would function in a closed – loop reservoir management setup is provided.

There are two important horizons in MPC as shown in Figure 3-1, both of which are expressed in terms of sampling instants. The prediction horizon is the span of time for which the plant outputs are predicted. The input horizon (or control horizon) is the number of control inputs that are calculated in the prediction computation, and is always smaller than the prediction horizon. In Figure 3-1, we could see that the prediction horizon is of 7 sampling time steps whereas the input horizon is only of 4 time steps.

The size of the prediction horizon is generally limited by computation speed; it is important to choose the control horizon such that the difference between the control and

prediction horizons is as least as long as it takes for all dynamics in the system to settle out.

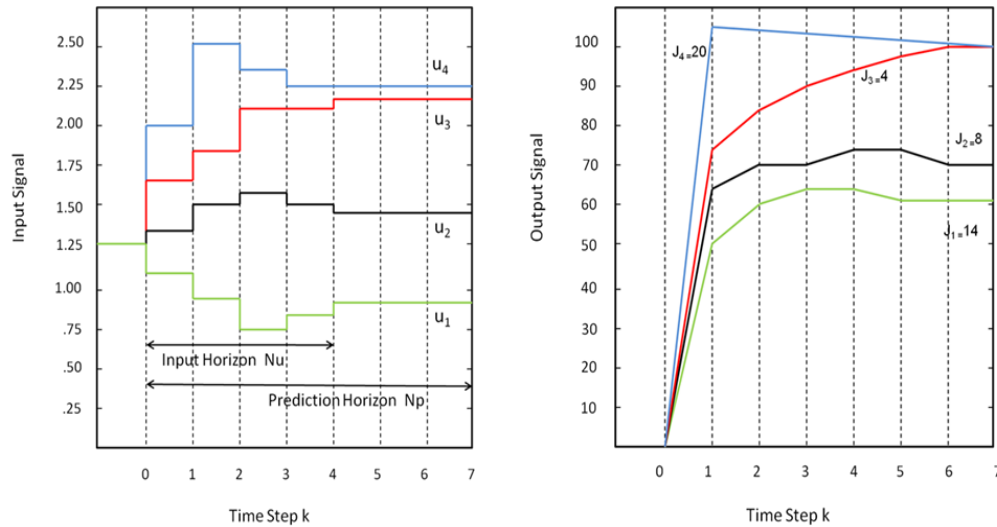


Figure 3-1 Receding Horizon Principle

For the current time step, $k=0$ the input $u = 1.25$ and the output $y = 0$. As shown in the input signal plot, the input horizon (N_u) is 4 sampling instants and the prediction horizon (N_p) is 7 sampling instants. Assume that the four input profiles u_1 , u_2 , u_3 , and u_4 are the possible input combinations to the reservoir, with their open loop dynamic responses y_1 , y_2 , y_3 , and y_4 as shown in the output signal plot. The desired output (set point) is 100. For each of the four cases we thus have the predicted output which was called as the open loop dynamic response and a reference trajectory which is the set point at 100.

3.2 The Cost Function

Any deviation of the predicted output from the set point trajectory is penalized by a cost function. The resulting cost function value for each of the four scenarios is given by J in Eq. 3.1. The form of the cost function indicates that it would be dependent on the weighted control input at each sampling instant over the input horizon as well as the weighted tracking errors at each sampling instant over the prediction horizon.

$$J = \sum_{j=1}^{N_u} \lambda_u \Delta u_j + \sum_{i=1}^{N_y} \lambda_e (y_{set} - y_{actual})_i \quad (3.1)$$

In this equation, J is the cost function, N_u is the control horizon, λ_u is the weight place on the changes in control, Δu is the change in input, N_y is the prediction horizon and λ_e is the weight placed on error.

3.3 The Constraints

If there was a constraint placed on the inputs that it could not be larger than 2.00, then u_3 and u_4 would no longer be a valid input, and only u_1 and u_2 would be considered as possible inputs. Similarly, if the outputs were constrained that it had to be less than 70 for instance, then u_2 , u_3 , and u_4 would no longer be valid inputs, since their output responses would be violating the specified output constraint. For such a case, u_1 would have to be chosen as the input even though it is not the optimal choice in the unconstrained case. Similarly, if a large weight was placed on the controller action in the cost function calculation; and a very small weight was placed upon the error, and then it

is possible that the cost function for u_I would be the minimum case and would be chosen as the command profile, even though the set point is never met for this case.

Thus, the careful selection of the tuning parameters and constraints is an integral part for any MPC implementation. A point to be noted is that the example illustrated focuses on a set point trajectory where the value of the set-point at any time $s(t) = 100$. This is the trajectory that the output has to follow ideally.

A variation of the set-point trajectory is the reference trajectory [21]. For the case discussed above, the reference trajectory would start at the current output $y(k)$ and would define an ideal trajectory along which the plant should return to the set-point trajectory. It can be set in such a way that the plant is to be driven back to the set point trajectory as fast as possible, but it is not always necessary. The reference trajectory therefore defines an important aspect of the closed-loop control of the behavior of the plant. For most cases it is assumed that the reference trajectory approaches the set-point by following an exponential trajectory from the current output value. The speed of the response is determined by the ‘time constant’ of the exponential which is denoted as TC .

4. INTRODUCTION TO SYSTEM IDENTIFICATION

With the underlying physics that govern the dynamics of the reservoir model, it is plain to see that the state equations grow to a substantial order. We would see that a typically high-order reservoir model would have the total number of variables in the order of $\mathcal{O}^5 - \mathcal{O}^7$ [12]. To reduce the complexity and computational cost involved in using the actual reservoir model in the controller design, we would need to extract the dominant behavior from these high order reservoir models and generate lower order models that would represent the reservoir model with a good accuracy. In other words we would need to perform an effective model order reduction step to mitigate the computational cost associated with the large scale model.

As discussed in the introduction, this reduction in the model order can be performed by generally two approaches. The mathematical reduction of the high-order system equation is called white-box modeling whereas recognizing the input-output behavior of the overall system and deriving a model that would imitate the same input –output behavior is called black-box modeling.

The focus of this Section will be directed at a Black-Box method called System identification. A background on identification theory and techniques will be provided before describing how we applied the System identification technique to identify a model representation of the reservoir model that could be used and an input to the MPC controller.

Subspace identification method includes elements from statistic, high-dimension geometry, linear algebra and system theory. Numerous papers on system identification

have been published over the last 40 years. The earliest work of this approach dates back to the 1960's [22], though substantial developments in the theory of stationary stochastic processes and multivariable statistical methods had taken place during the 1950's. The theory got serious attention and was widely recognized in the late 80's, showing promising results through the work of Willems [23] [24], De Moor [25], Moonen [26], Van Overschee [16]. One of the most significant contributions was in the last decade when Van Overschee and De Moor had published a first comprehensive book on subspace identification of linear systems [17].

4.1 The Black Box Model

Figure 4-1 shows the schematic diagram of the black box system with input u_k , output y_k and disturbance v_k . Here we will observe the inputs and outputs but not the disturbances. We can manipulate the input u_k but not the output y_k .

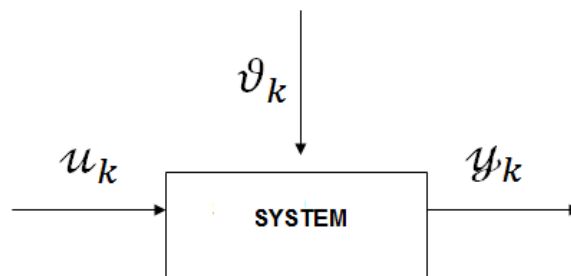


Figure 4-1 Schematic of Black Box Model

Even if we do not know the internal structure of the system mathematically, the measured output and input data would provide us useful information about the behavior of the system. With this information, we will be able to construct mathematical models

to describe the dynamics of the system from the observed output-input data. This method called as the black-box approach. Our primary goal is to retrieve to correct output from a given signal input.

4.2 An Overview of the Theory

The mathematical model used for system identification purposes in this thesis is from Van Overschee and De Moor [17]. The subspace identification are concerned with systems and models of the form

$$\begin{aligned}x_{k+1} &= Ax_k + Bu_k + w_k, \\y_k &= Cx_k + Du_k + v_k\end{aligned}$$

where

$$E \left[\begin{pmatrix} w_p \\ v_p \end{pmatrix} \begin{pmatrix} w_p^T & v_p^T \end{pmatrix} \right] = \begin{pmatrix} Q & S \\ S^T & R \end{pmatrix} \delta_{pq} \geq 0$$

Here, w_k , is called the process noise and v_k is the measurement noise. It is assumed that they are zero mean. For our case, we can assume them to be zeros as we are getting our inputs and outputs directly from the reservoir simulator in which we had not considered noise as such. A is the system matrix, B is the input matrix, C is the output matrix and D is the direct feed-through matrix which were described in the previous Section. The matrices Q , S and R are the covariance matrices of the noise sequence.

The main problem treated would be that- given the input and output measurements, we need to find and approximate system of order n and estimate the

system matrices A , B , C , D , Q , R and S . De Moor [25] had suggested the input-output relationship for linear systems based upon the following equation,

$$Y_f = \Gamma_i X_i + H_i^d U_f + H_i^s M_f + N_f \quad (4.1)$$

This equation played a very important role in the development of subspace identification. The different terms in Eq. 4.1 can be defined as;

$$\Gamma_i = \begin{pmatrix} C \\ CA \\ CA^2 \\ \vdots \\ CA^{i-1} \end{pmatrix},$$

is the extended observability matrix. The deterministic lower block triangular Toeplitz matrix is defined as

$$H_i^d = \begin{pmatrix} D & 0 & 0 & \dots & 0 \\ CB & D & 0 & \dots & 0 \\ CAB & CB & 0 & \dots & 0 \\ \vdots & \vdots & \vdots & \vdots & \vdots \\ CA^{i-2}B & CA^{i-3}B & CA^{i-4}B & \dots & 0 \end{pmatrix},$$

The stochastic lower block triangular Toeplitz matrix is given as;

$$H_i^s = \begin{pmatrix} 0 & 0 & 0 & \dots & 0 \\ C & D & 0 & \dots & 0 \\ CA & C & 0 & \dots & 0 \\ \vdots & \vdots & \vdots & \vdots & \vdots \\ CA^{i-2} & CA^{i-3} & CA^{i-4} & \dots & 0 \end{pmatrix},$$

The input block Hankel matrix is defined as;

$$U_{a|b} = \begin{pmatrix} u_a & u_{a+1} & \dots & u_{a+j-1} \\ u_{a+1} & u_{a+2} & \dots & u_{a+j} \\ \vdots & \vdots & \vdots & \vdots \\ u_b & u_{b+1} & \dots & u_{b+j-1} \end{pmatrix},$$

A similar definition is there for the output Hankel matrix. The subscript j is the size of the data set that we perform system identification on. This is assumed to be large ($j \rightarrow \infty$). The subscripts a and b denotes the discrete time steps. (As far as the data is concerned, we used an in house simulator developed in Matlab® for prototyping the equations and algorithms, but used a commercial software called Eclipse® to obtain more realistic data). Also defined for convenience and short hand notation are;

$$U_p = U_{0|i-1}, \quad U_f = U_{i|2i-1},$$

$$Y_p = Y_{0|i-1}, \quad Y_f = Y_{i|2i-1},$$

where the subscripts p and f denote, the past and future respectively. These matrices are paired and stacked in two new matrices given as;

$$W_t = \begin{pmatrix} Y_t \\ U_t \end{pmatrix}, \quad t = p, f,$$

The block Hankel matrix formed with the process and measurement noise are defined similarly as

$$M_p = M_{0|i-1}, \quad M_f = M_{i|2i-1},$$

$$N_p = N_{0|i-1}, \quad N_f = N_{i|2i-1},$$

We finally denote the state sequence as

$$X_i = (x_i \quad x_{i+1} \quad x_{i+2} \quad \dots \quad x_{i+j-1})$$

Definition: If A and B are two matrices spanning a row space, then the orthogonal projection of the row space of A into the row space of B is denoted by A/B which is defined as

$$A/B = AB^\dagger B.$$

A/B^\perp is the projection of the row space of A into B^\perp , for which we have

$$A/B^\perp = A - A/B$$

The orthogonal projection of the future outputs Y_f into \mathbf{U}_f^\perp is given as

$$Y_f/\mathbf{U}_f^\perp = \Gamma_i X_i/\mathbf{U}_f^\perp + H_i^S M_f/\mathbf{U}_f^\perp + N_f/\mathbf{U}_f^\perp$$

Since it is assumed that the noise is uncorrelated with the inputs we have that:

$$Y_f/\mathbf{U}_f^\perp = \Gamma_i X_i/\mathbf{U}_f^\perp + H_i^S M_f + N_f$$

When we multiply this equation with two weighting matrices W_1 and W_2 that satisfies the following three conditions;

$$\text{rank}(W_1 \cdot \Gamma_i) = \text{rank} \Gamma_i,$$

$$\text{rank} X_i = \text{rank}(X_i/\mathbf{U}_f^\perp \cdot W_2),$$

$$W_1 \cdot (H_i^S M_f + N_f) \cdot W_2 = 0.$$

we get

$$\begin{aligned} \mathcal{O}_i &= W_1 \cdot X_i/\mathbf{U}_f^\perp \cdot W_2 \\ &= W_1 \cdot \Gamma_i X_i/\mathbf{U}_f^\perp \cdot W_2. \end{aligned} \tag{4.2}$$

By singular value decomposition (SVD), we can now state the properties

$$\text{rank} \mathcal{O}_i = n$$

$$W_1 \cdot \Gamma_i = U_1 S^{1/2},$$

$$X_i/\mathbf{U}_f^\perp \cdot W_2 = S^{1/2} V_2^T,$$

where

$$\mathcal{O}_i = (U_1 \quad U_2) \begin{pmatrix} S & 0 \\ 0 & 0 \end{pmatrix} \begin{pmatrix} V_1^T \\ V_2^T \end{pmatrix}$$

Since there are different possibilities for the choices of W_1 and W_2 , there are as many variations in subspace implementation. The remaining shows the basic step of how system matrices can be found. The approach described here was used in this thesis for obtaining the system matrices of the reservoir models. In this case, the inputs and outputs were obtained from a reservoir simulator.

In the following, the estimated state sequence \hat{X}_i is the Kalman filter estimate of X_i (Van Overschee and De Moor, [17]). The projection into Eq. 4.2 leads to the sequence;

$$\begin{aligned} \mathcal{O}_i &= W_1 \cdot Y_{i+1|2i-1} / U_{i+1|2i-1}^\perp \cdot W_2 \\ &= W_1 \cdot \Gamma_{i-1} \hat{X}_{i+1} \cdot W_2. \end{aligned}$$

The state space matrices can now be found by solving a simple set of over determined equations in a least square sense;

$$\begin{pmatrix} \hat{X}_{i+1} \\ Y_{i|i} \end{pmatrix} = \begin{pmatrix} A & B \\ C & D \end{pmatrix} \begin{pmatrix} \hat{X}_i \\ U_{i|i} \end{pmatrix} + \begin{pmatrix} \rho_w \\ \rho_v \end{pmatrix}.$$

By the definition for \mathcal{V}_w and \mathcal{V}_v as residual matrices, this reduces to;

$$\min_{A,B,C,D} \left\| \begin{pmatrix} \hat{X}_{i+1} \\ Y_{i|i} \end{pmatrix} - \begin{pmatrix} A & B \\ C & D \end{pmatrix} \begin{pmatrix} \hat{X}_i \\ U_{i|i} \end{pmatrix} \right\|_F^2,$$

The noise covariances Q , S , and R can be estimated from the residuals as;

$$\begin{pmatrix} Q & S \\ S^T & R \end{pmatrix}_i = \frac{1}{j} \left[\begin{pmatrix} \mathcal{V}_w \\ \mathcal{V}_v \end{pmatrix} \cdot \begin{pmatrix} \mathcal{V}_w^T & \mathcal{V}_v^T \end{pmatrix} \right] \geq 0.$$

For a more detailed study on this, the book by (Van Overschee and De Moor, [17]) is recommended. With this we can conclude the brief summary of the theory behind system identification. Now let us look at an implementation of the same for a particular case.

4.3 An Example - 2D Homogeneous Reservoir

In order to apply the subspace identification framework to reservoir simulation, we chose the reservoir model as depicted in Figure 4-2. This reservoir is simple enough yet, at the same time, realistic for understanding the procedures that are performed for subspace identification. The reservoir has similar rock properties everywhere. The reservoir and rock properties are as shown in Table 4-1.

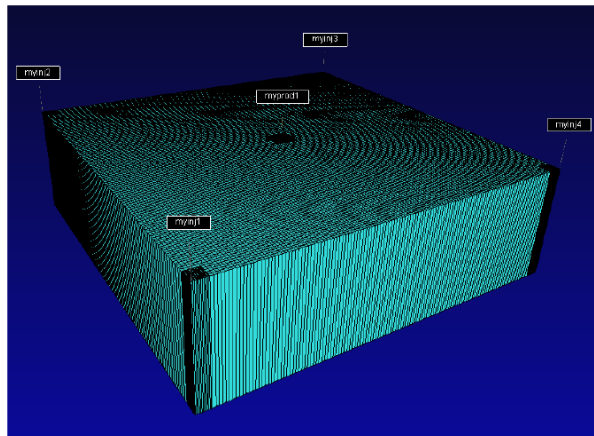


Figure 4-2 2D Homogeneous Reservoir

The term “2D” stems from that fact that the reservoir is meshed with just one layer. In other words, this would mean that the fluid does not move vertically. The reservoir has 51 x 51 number of grid blocks and we assume a two-phase flow in the reservoir. There are four producers located in the corners and one producer in the center.

Table 4-1 Reservoir and Fluid Properties for System-ID

Variable	Description	Value	Unit
ρ_o	Density of Oil	45.0	lbm/ft ³
ρ_w	Density of Water	62.0	lbm/ft ³
μ_o	Viscosity of Oil	10	cp
μ_w	Viscosity of Water	.89	cp
c_o	Compressibility of Oil	$10 \cdot 10^{-6}$	psi ⁻¹
P_o	Initial Pressure	3800	psia
S_o	Initial Saturation	0.1	[-]
ϕ	Rock Porosity	.20	[-]

4.3.1 Experimental Design

One of the major steps involved in the system identification is to design the various tests needed to perform in order to come up with the best input signal that would help capture and represent all the dynamics of the original system in the state-space model generated. When a study was conducted on the literature that was available on subspace identification, it was noticed that the focus was mainly on the various identification algorithms than to the design of the experiments. In order to find the characteristics of the process outputs, an important experiment called the stair-case experiment [27] needs to be performed. It is done to design the input signal that will be used to perform system identification for the reservoir. Some important characteristics can be studied using this test. They are:

- The linearity range of the process
- The estimation of the time constant.

It is important to estimate the time constant because with this, we can determine the duration of the system identification signal. After calculating the time constant “T”, we can estimate the bandwidth frequency of the system (Hz) as “1/T”. Thus by conducting the experiment till about 5 – 10 times the duration of the time constant we will be able to capture the important input-output behavior of the real reservoir.

Another important aspect to be considered is the amplitude of the input steps. The amplitude mainly depends on the noise ratio and the linearity range. As far as noise is concerned, since we are just dealing with computer generated inputs and outputs, we can neglect the effect of noise on amplitude. However, it is important to maintain the system well within the linearity range.

The stair case experiment was thus conducted for various injection rates. The motivation was to find out the upper limit of the injection rate that would still ensure that the system outputs change linearly. From Figure 4-3, it could be seen that linearity is assured by injecting at rates up to 1200 BBL/day. If the injection rate was beyond this level, the output – which is the oil production, would exhibit a sudden change in rate thus hinting us that the linearity is lost.

We also need to limit the input design in such a way that we could capture the most important dynamics taking place in the system. After characterizing the various parameters, the step signal was constructed in Matlab. The total duration for maintaining a constant step was determined mainly by analyzing the time constant (the time by the system to reach 63 % of its final value in a step response [27]). The staircase experiment could be considered to be a form of step response by itself.

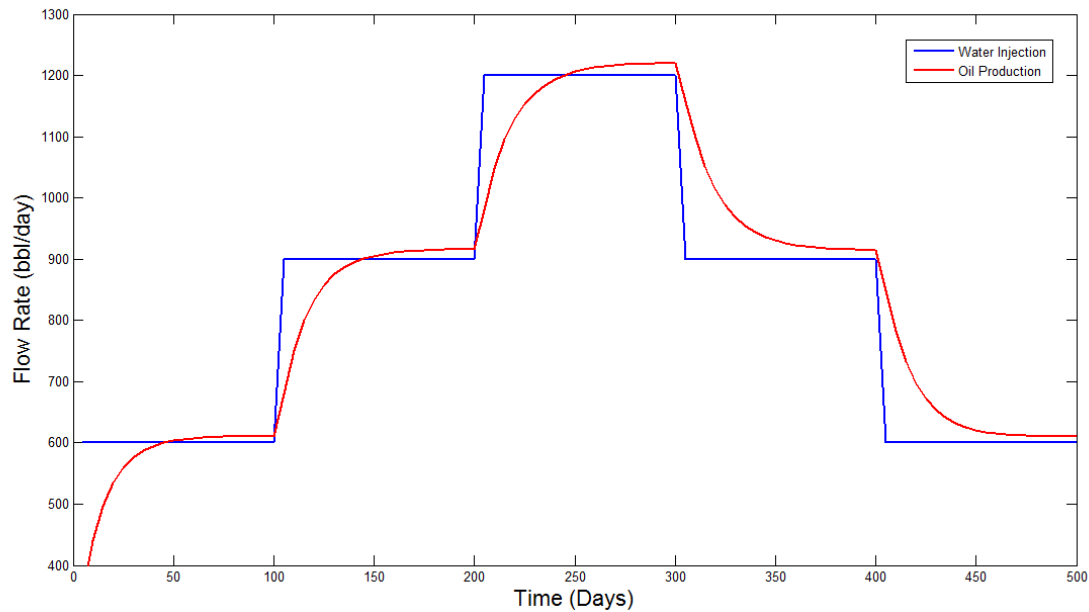


Figure 4-3 Staircase Experiment

Using this time constant, we can compute the system bandwidth frequency (ω_b). The information obtained from the staircase experiment suggests a system bandwidth frequency that is equal to 0.1 rad/sec. This is computed as being equal to $1/\tau$, where τ is the time constant.

The sampling frequency (ω_s) for the input signal, is another important aspect that needs to be decided. From the system bandwidth (w_b) already calculated, we can approximate the sampling frequency to be between $10w_b < w_s < 30w_b$.

After we decided the approximate input signal, the next was to identify the model. The Figure 4-4 shows the input signal that was initially applied to the model and Figure 4-5 shows the output that was obtained. As we could see, this is a RBS (Robbed Bit

Signal) that was applied to the injector well that fluctuates between 300 BBL/day and 600 BBL/day. As was already inferred from the staircase experiment, this range of inputs is well within the linearity range of the reservoir model. The RBS signal was applied for 100 days because this was decided as a decent experiment length based upon the calculation of the time constant and system bandwidth done before.

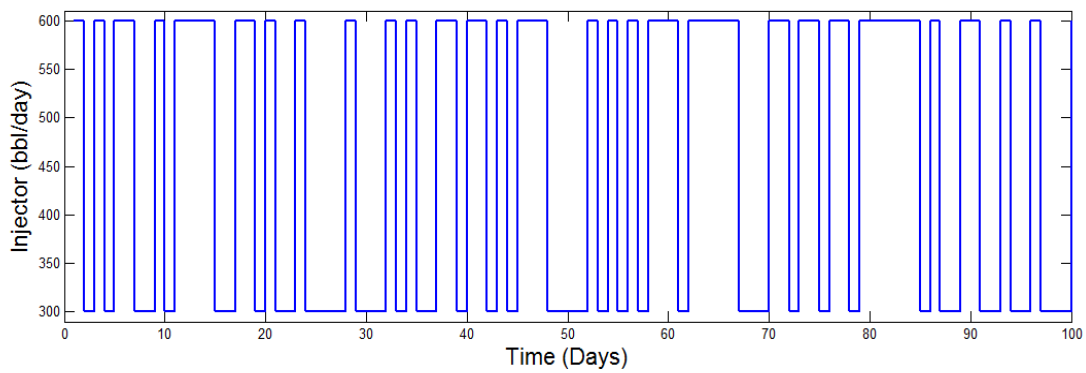


Figure 4-4 Input Signal

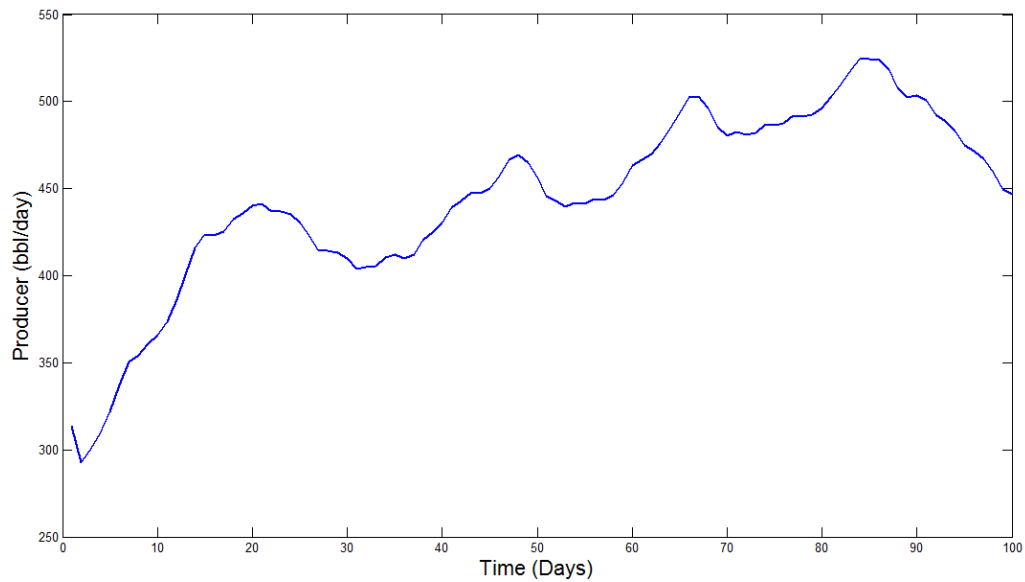


Figure 4-5 Output Obtained

When the same inputs were provided to the actual reservoir model in order to compare the output quality of the identified model, a very good simulation fit was obtained as shown in Figure 4-5.

The simulation fit was measured using the following formula

$$\text{Simulation fit} = \frac{1 - \epsilon_i^{\max}}{1} \times 100\%,$$

where

$$\epsilon_i^{\max} = \max |(\bar{Y}_i - \hat{Y}_i) / \bar{Y}_i|, \quad i \in \{1, \dots, 4\}$$

Here, \bar{Y}_i is the output as measured from the actual reservoir model; \hat{Y}_i is the output obtained from the identified model by using system identification. The equation first calculates the maximum relative error for each of the outputs (from the four production wells) over the time period and then plugs this value in the simulation fit equation. The simulation fit shown in Figure 4-6 was calculated to be 95.3%.

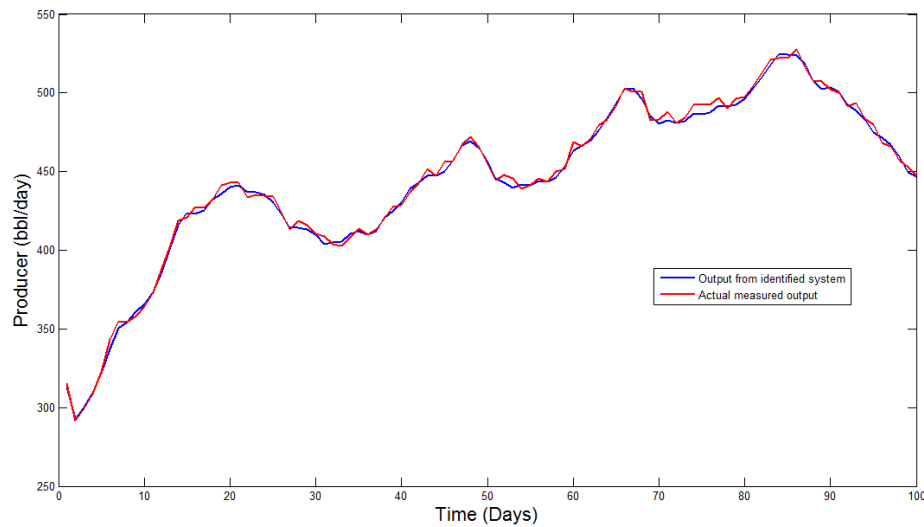


Figure 4-6 Simulation Fit

4.3.2 Model Validation

The interest now lies in finding if the model that was just identified had the ability to predict the outcome of the some input sequence other than the identification sequence. A simulation fit of 90.6% was obtained in this case. This is a pretty decent fit as could be seen in Figure 4-7. It needs to be noted that we performed subspace identification with order 5 . Identification was done on an reservoir simulator model with grid cells 51 x 51. The full order model is of size 5202 x 5202. This is a measure of the size of the state space input matrix if no reduction is performed. That would mean that we are dealing with a system of order 5202. The order of the identified model is only 5. Thus there is a significant decrease in computational effort when using an identified model instead of the actual reservoir model.

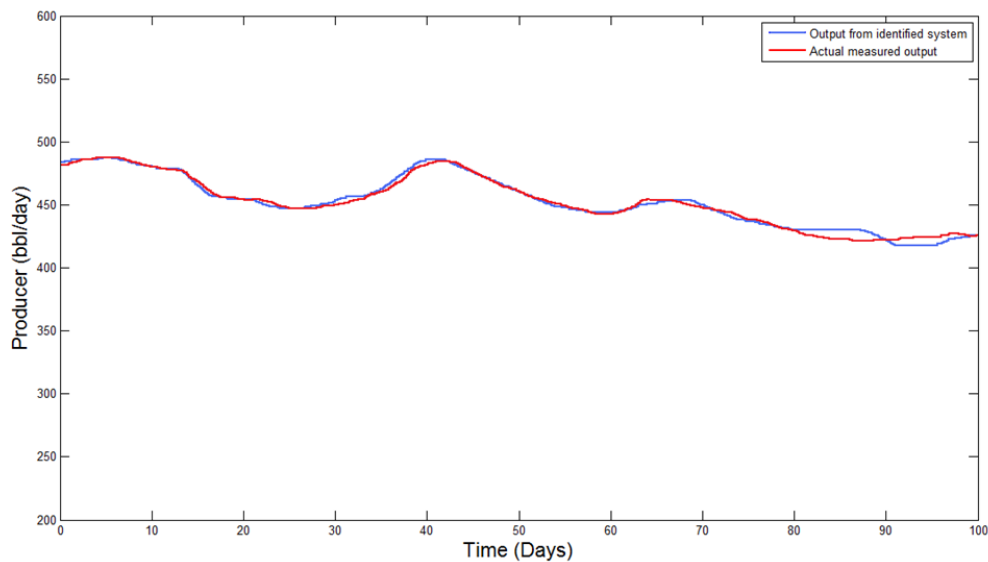


Figure 4-7 Model Validation Fit

4.3.3 An Expanded Model

In the previous Section, we have recognized the ability of the model to track the output effectively when an input sequence that was different from the identification sequence was used. Our next aim would be to verify if this model could satisfactorily predict the outputs accurately for periods beyond the identification time. Assuming that the actual dynamics within the reservoir wouldn't change drastically (especially by some means of non-linear dynamics that can occur as a result of water breakthrough in any of the wells) we would want to have an idea about how long can the model provide a good prediction quality, in order to decide, when we would want another system identification to be performed.

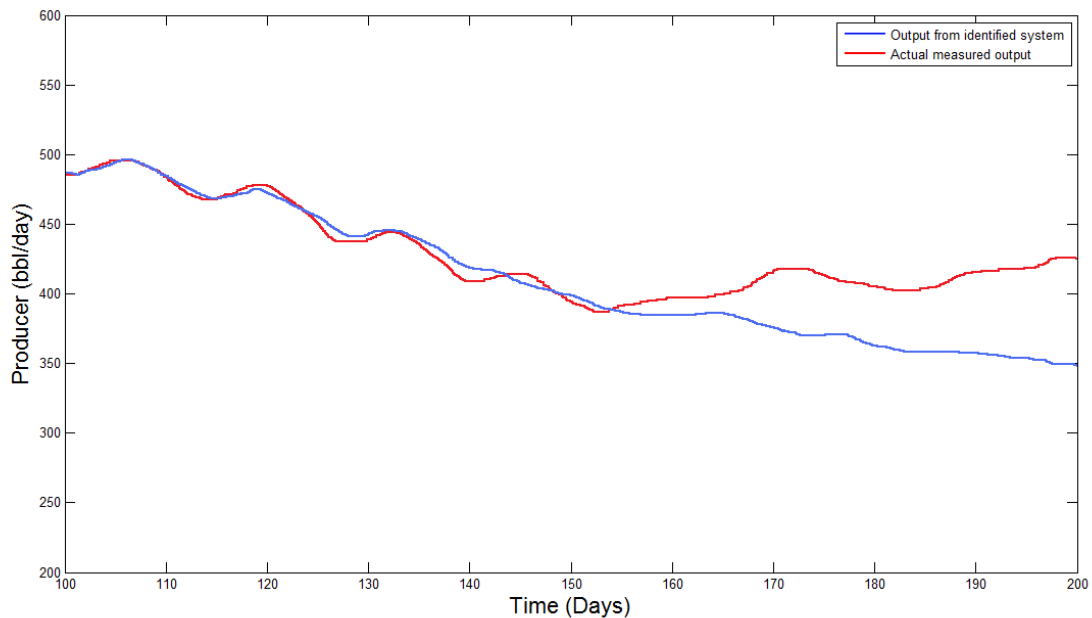


Figure 4-8 Expanded Model Fit

For the early stages of the reservoir Figure 4-8 shows that we could derive a good model that could track the output pretty well. Beyond 140 days, we could also recognise

a significant drop in the model quality. This would suggest that a system re-identification would be necessary at about 140 days. Moreover, the early stages of the reservoir represents a special simpler case of the reservoir model with no water cut at any of the producing wells. The reason why the system identification fails to maintain model quality beyond 140 days could also be attributed to the fact that the model might be experiencing some additional nonlinear dynamics due to the appearance of water in the producers. The Section 6 to follow would discuss two cases where system identification has been performed in a similar fashion but with the intention of performing production optimization.

5. MPC AND SYSTEM-ID – APPLIED TO RESERVOIR SIMULATION

In this Section we will be putting together MPC and System-ID to control the dynamics of the waterflooding process. For reasons of simplicity, we focus our attention to reservoir with only oil and water present. In other words, this means that we are considering only two phase flow in the reservoir. The diagram shown below is a pictorial representation of the waterflooding processes in the 2D reservoir model with a horizontally placed water injection that runs across the left corner of the reservoir, and a horizontally placed production well that runs across the right of the reservoir. There are Internal Control Valves (ICVs) that are placed at regular intervals all across the horizontal length of the injection and production wells. These valves are placed so that we can have independent control over the injection flow rates across the length of the reservoir.

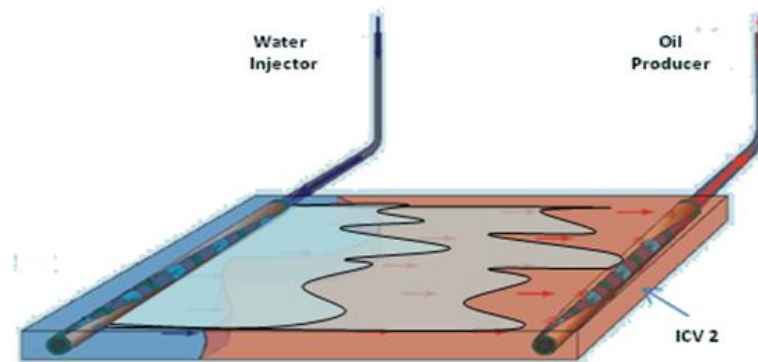


Figure 5-1 Open-Loop Waterflooding (adapted from [2])

When water is injected, it travels through the reservoir, away from the injection wells, but not in a uniform manner. This is because of the strong heterogeneous nature of the reservoir rock. It could be noticed that the water front has an irregular shape as

makes its path towards the production side of the reservoir. This phenomenon is called as the fingering effect. This can be attributed mainly to the fact that in certain parts of the reservoir, the fluids experience lesser resistance and hence the water front moves much faster at that local region.

Once the waterfront has reached the production side of the reservoir, as a result of this fingering effect, particular regions across the length of the horizontal well would experience a significant increase in the production of water. Thus the water production through some of ICV's (ICV number two as shown in Figure 5-1) would become significantly high. This would in turn result in a high water production from the whole well as such, (typically more than 90% water production), and the production well would have to be closed (shut in).

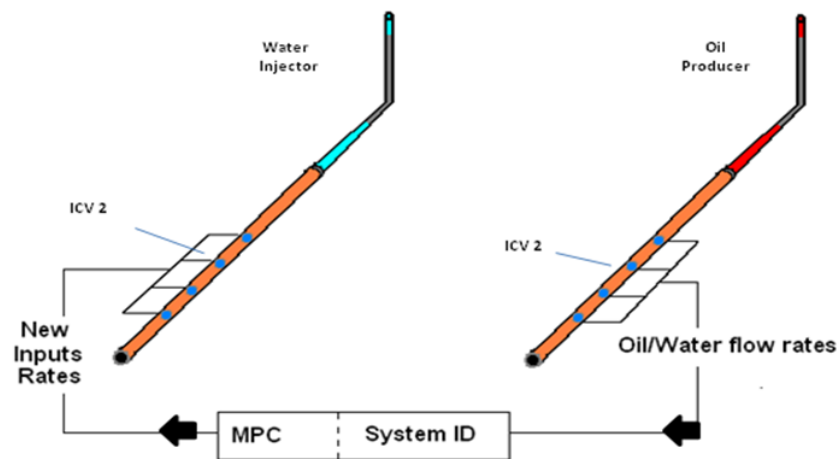


Figure 5-2 Proposed Controller for Waterflooding

What we would ideally want is a water front that uniformly progresses across the width of the reservoir without being affected by the heterogeneity in the reservoir. For this to happen, we would like to have independent control over the downhole ICVs at the

injection side as well as the production side. Using these valves, the amount of water injected into the reservoir and oil produced from specific portions of the production well can be controlled. This control ability is what we wish to achieve by integrating MPC and System-ID with the reservoir model as shown in Figure 5-2.

The inputs and outputs measured at the injection and production side would be used to perform a system identification of the reservoir model. After the model has been correctly identified, this identified model would be used in the MPC control algorithm to generate the new inputs (which could be the injection rates and production bottom hole pressures or injection bottom hole pressures and production rates; depending on what we decide to control and what we decide to measure).

In this manner we would be able to establish a control at the individual ICV level and thereby have an indirect control over the propagation of the water front. By the use to these “intelligent” or “smart” wells, we could ensure that the reservoir is depleted uniformly throughout when the waterfront reaches the production side of the reservoir. This would obviously ensure a high net present value (NPV) and a high ultimate oil recovery.

5.1 The Dynamic Control Capability

Earlier in the Section an elaborate explanation was provided on the “Receding Horizon Principle” (see Figure 3-1) of the MPC controller. Here, let us see how an MPC controller would function in a reservoir simulator setting.

Assume that the System-ID was already been performed and that we have an identified reservoir model that could be used for MPC implementation. Let the MPC controller have a prediction horizon (or output horizon) of nine time-steps and an input (or control) horizon of 5 time-steps as shown in Figure 5-3. We wish to control the rate at the injection well by having a control over the valve's opening and closing. The bottom-hole pressures at the ICVs present at the production well is what we intend to measure as the output. We also assume a discrete setting, and that the current time is labeled as time step 0. For our case, we will be dealing with the internal model that is linear and strictly proper. (This means that the calculation of the best input would be straight forward and the output $y(k)$ would only depend on the past inputs $u(k-1)$, $u(k-2)$, but not on the input at (k) .)

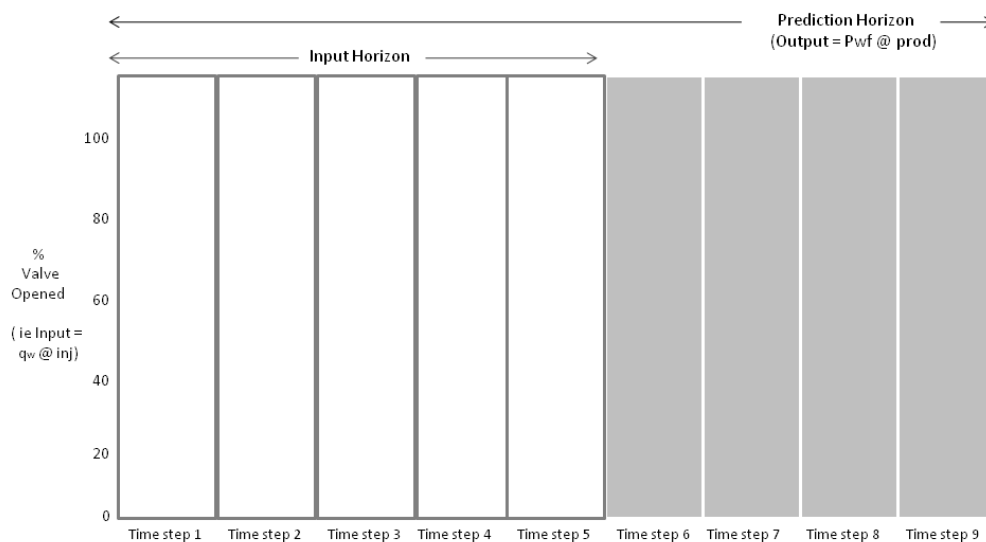


Figure 5-3 MPC as Applied to Waterflooding Control - a

At the first time step, say we decided on the input trajectory as shown in Figure 5-4, based upon our optimization objectives and constraints from the formulated optimization problem. In the simplest case, we can try to formulate the optimization problem to choose the input trajectory so that the output follows its reference trajectory (this is not shown in figure). The predicted behavior of the outputs will be dependent on the assumed input trajectory $\hat{u}(k + i|k)(i = 0, 1, \dots, H_p - 1)$ that has been computed at the time k . The input were calculated for each time step in the input horizon. This would mean that the inputs for the 5 time steps in the future has already been calculated eventhough the output measurements are available only till the present time step (which is one).

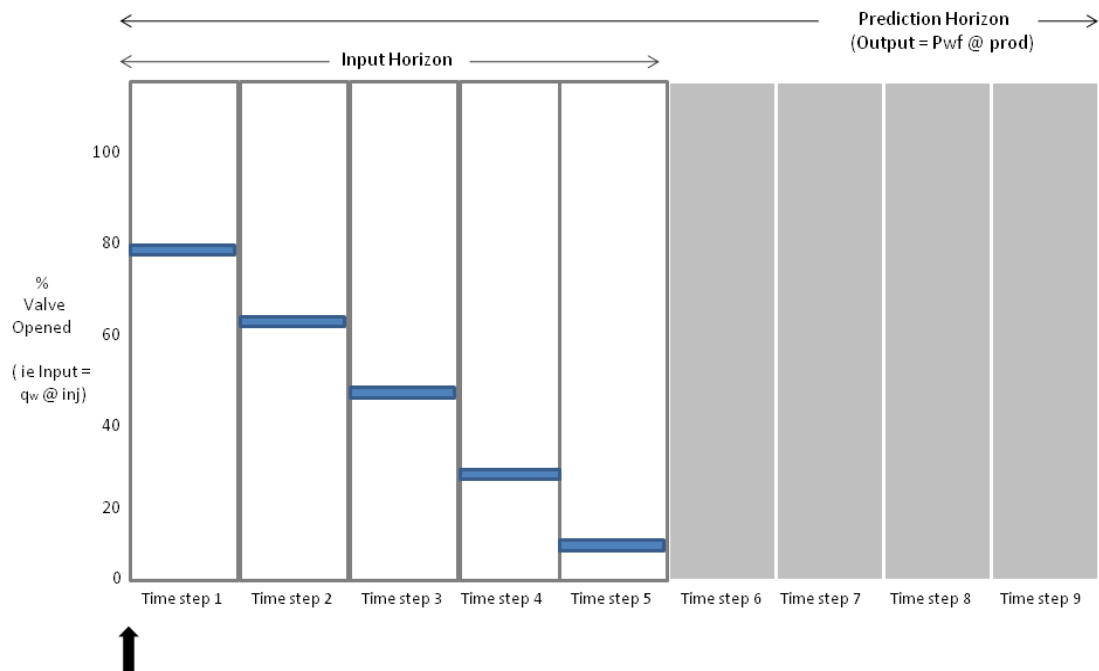


Figure 5-4 MPC as Applied to Waterflooding Control - b

The input trajectory suggests that the well be almost completely closed within the next five time steps. This may be because of significant increase in water production at the ICV in the production well. Once the future input trajectory was chosen, only the first element of that trajectory is applied as the input to the reservoir as shown in Figure 5-5. At the present time k , this would mean that we set our actual applied signal $u(k)$ to be equal to $\hat{u}(k/k)$ – which denotes the first element of the computed input trajectory.

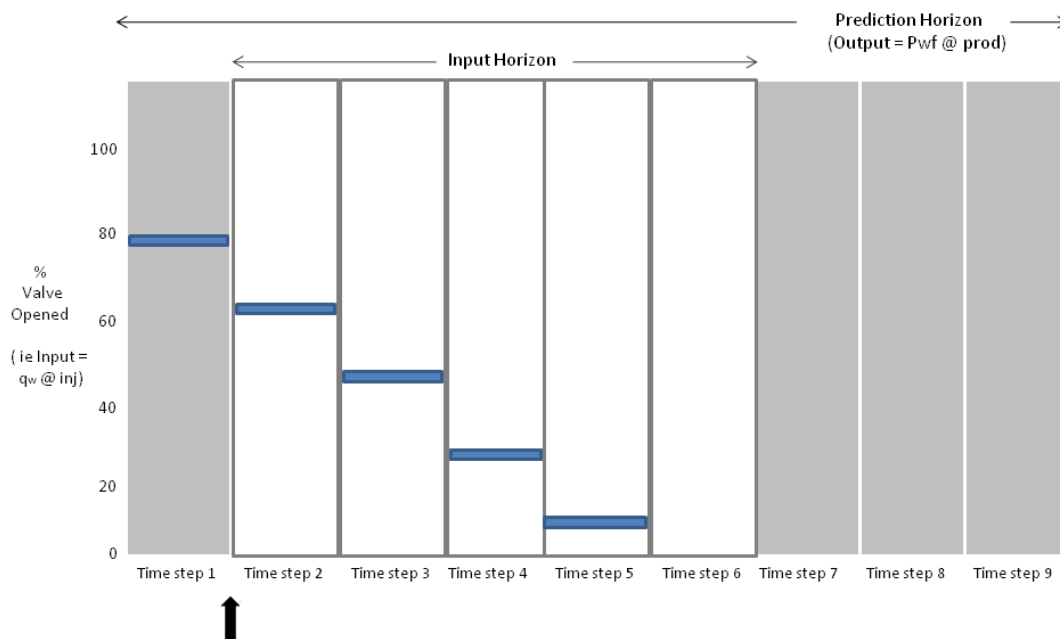


Figure 5-5 MPC as Applied to Waterflooding Control – c

We then progress in time ready for the next cycle of events. Then we repeat the complete cycle of output measurement, prediction, and input trajectory determination, for the next sampling instant and then a completely new output measurement $y(k + 1)$; a new reference trajectory $r(k + i|k + 1)(i = 2,3 \dots)$ is obtained. Predictions are made

over the horizon $(k + 1 + i)$, with $i = 1, 2, \dots, H_p$ and a new input trajectory $\hat{u}(k + 1 + i|k + 1)$, with $i = 0, 1, \dots, H_p - 1$ is chosen as shown in Figure 5-6.

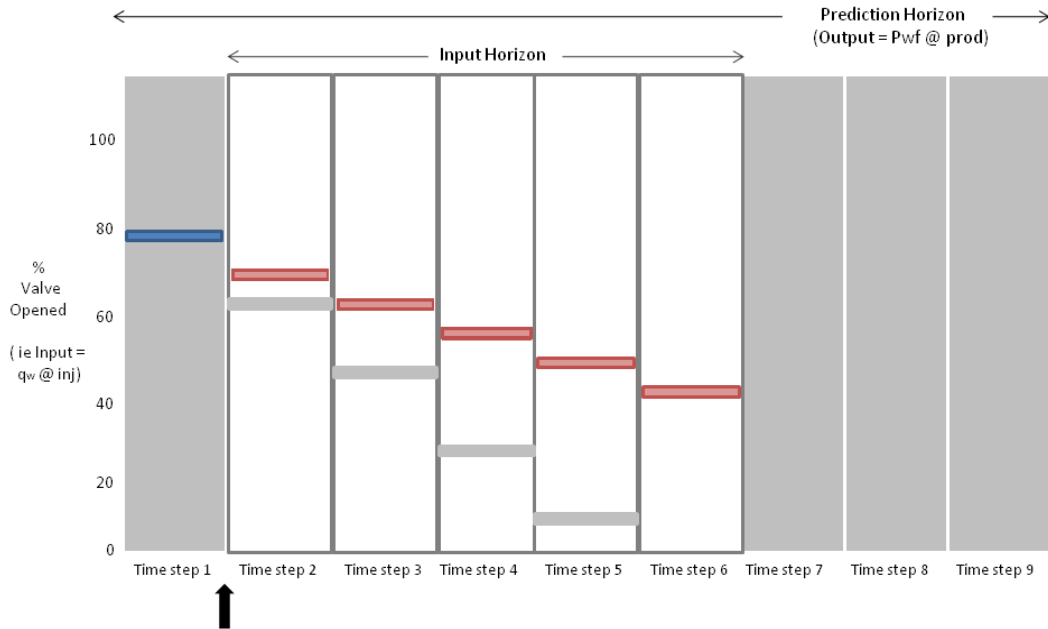


Figure 5-6 MPC as Applied to Waterflooding Control - d

Again we select the first element of the new input trajectory i.e. $u(k + 1) = \hat{u}(k + 1|k + 1)$ as shown in Figure 5-7.

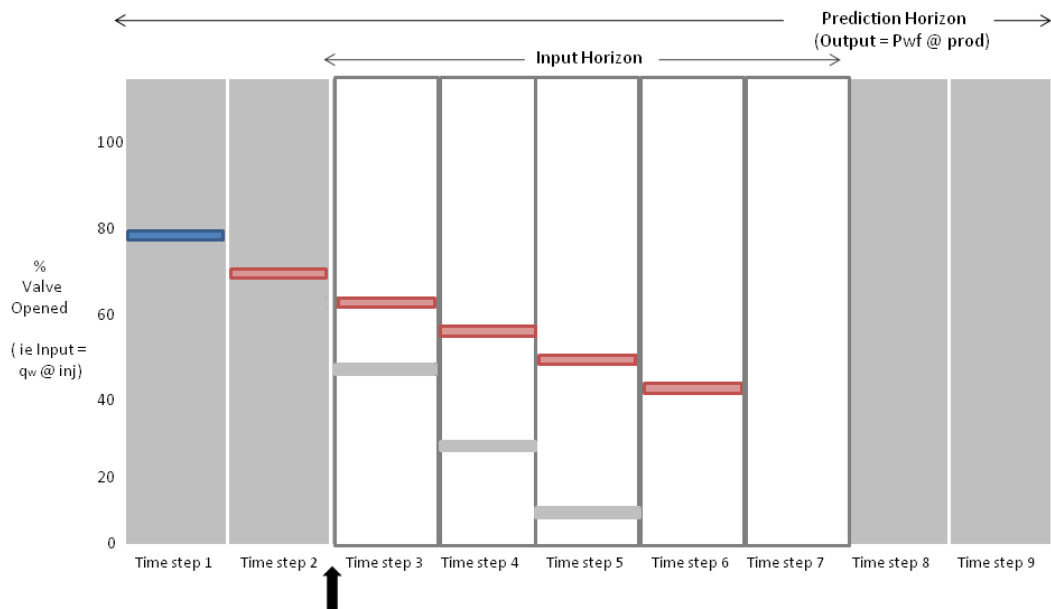


Figure 5-7 MPC as Applied to Waterflooding Control - e

and progress another step in time as illustrated in Figure 5-8. This process we repeat for each time step.

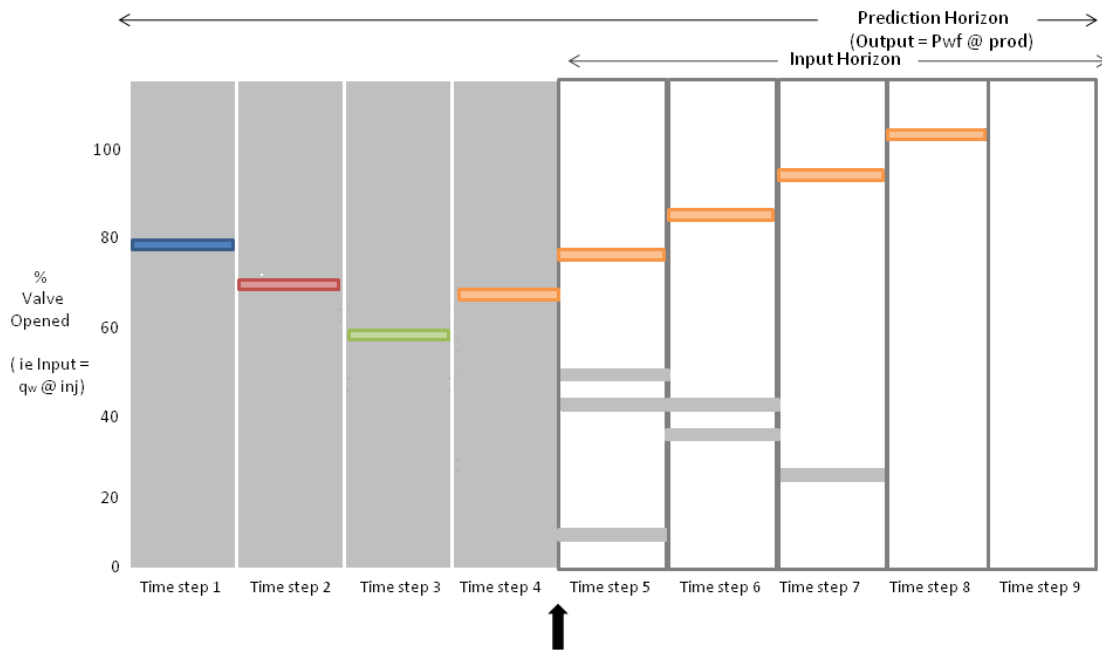


Figure 5-8 MPC as Applied to Waterflooding Control - f

Since the prediction horizon always remains of the same length and moves ahead in time at each sampling instant, this way of controlling a plant is often called a receding horizon strategy. At the end of the life cycle of the reservoir, we could clearly that control strategy resulted in a dynamic control of the inputs, taking into consideration the outputs, reference trajectories, prediction, objective function and constraints for each and every time step.

5.2 The Formulation of the MPC Control Problem

We would basically need to take care of three tasks in formulating an MPC control problem. The first of which would be to come up with the plant model on which we will be performing our control operations. This task would be carried out by performing system identification on the real reservoir model. This step was already explained in Section 4.

With this, we will be able to get the identified model with the following identified state-space formulation;

$$\begin{aligned}x(k + 1) &= Ax(k) + Bu(k) \\y(k) &= C_y x(k) \\z(k) &= C_z x(k)\end{aligned}$$

The second task would be to formulate the cost function or objective function which we would be interested in optimizing. The cost function is quadratic and its formulation is done two different ways in this thesis. Both these case will be analyzed interpreted in the Section to follow.

In the first type of formulation is dependent on the predicted controlled outputs and the reference trajectory that our outputs have to follow. It can either be defined as the penalty for the deviations of the predicted controlled outputs form the reference trajectory as the following equation suggests.

$$V(k) = \sum_{i=H_w}^{H_p} \|\hat{z}(k + i|k) - r(k + i|k)\|_{Q(i)}^2 + \sum_{i=0}^{H_u-1} \|\Delta\hat{u}(k + i|k)\|_{R(i)}^2 \quad (5.1)$$

Here, $\hat{z}(k)$ is the vector of outputs which are to be controlled, and $Q_{(i)}$ and $R_{(i)}$ accounts for the penalty weights in states and control prediction respectively. The

prediction horizon has the length H_p , the input horizon is of length H_u , and we start penalizing the deviations of z from r from the H_w time step. This is to say that the error vector $\hat{z}(k+i|k) - r(k+i|k)$ is penalized at every point in the prediction horizon, in the range

$$H_w \leq i \leq H_p$$

The form of the cost function also suggests that there is a cost involved in the change in control input $\Delta\hat{u}$. It needs to be pointed out that in this formulation of cost function, we are not penalizing the particular values of the input vector $u(k)$, but only the changes in the input vector. This decision might differ on a case to case basis.

The other type of formulation is to maximize the oil production rates from all the producers. For instance, let us assume that we are interested in maximizing the production through only two production wells. Then for this case the objective function would mathematically take the form;

$$V(k) = \sum_{i=0}^{H_u-1} (q_i^{P_1})^2 + (q_i^{P_2})^2 \quad (5.2)$$

Both these forms of cost functions (Eq. 5.1 and Eq. 5.2) should be rewritten in terms of $\Delta\hat{u}$ which is the variable in which we would formulate our optimization problem (since $\Delta\hat{u}$ is the control variable) as;

$$\begin{aligned} V(k) &= \sum_{i=0}^{H_u-1} \hat{u}_j^T H \hat{u}_j \\ &= \begin{bmatrix} \hat{u}_{k|k} \\ \vdots \\ \hat{u}_{k+H_u-1|k} \end{bmatrix}^T \begin{bmatrix} H & \cdots & 0 \\ \vdots & \ddots & \vdots \\ 0 & \cdots & H \end{bmatrix} \begin{bmatrix} \hat{u}_{k|k} \\ \vdots \\ \hat{u}_{k+H_u-1|k} \end{bmatrix} \end{aligned}$$

$$\begin{aligned}
&= \mathcal{U}(k)^T \mathcal{H} \mathcal{U}(k) \\
&= \|\mathcal{U}(k)\|_{\mathcal{H}}^2 \\
&= \|A_{u_k} u_{k-1} + B_{u_k} \Delta \mathcal{U}(k)\|_{\mathcal{H}}^2
\end{aligned}$$

The inputs $\mathcal{U}(k)$ can be written in terms of $\Delta \mathcal{U}(k)$ as $\mathcal{U}(k) = A_{u_k} u_{k-1} + B_{u_k} \Delta \mathcal{U}(k)$.

(5.3)

$$= \frac{1}{2} \mathcal{U}(k)^T \hat{\mathcal{H}} \mathcal{U}(k) + \Delta \mathcal{U}(k)^T f + K(u_{k-1}),$$

where,

$$\begin{aligned}
\hat{\mathcal{H}} &= 2B_{u_k}^T \mathcal{H} B_{u_k}, \\
f &= 2B_{u_k}^T \mathcal{H} A_{u_k} u_{k-1}, \\
K(u_{k-1}) &= u_{k-1}^T A_{u_k}^T \mathcal{H} A_{u_k} u_{k-1},
\end{aligned}$$

Eq. 5.3 shows the objective function in its final reduced form.

The last step is the formulation of the constraints. Considering to the objective function above, the corresponding optimization problem would have its constraints represented in one of the following methods

$$E \text{vec}(\Delta \hat{u}(k|k), \dots, \Delta \hat{u}(k + H_u - 1|k), 1) \leq \text{vec}(0)$$

$$F \text{vec}(\hat{u}(k|k), \dots, \hat{u}(k + H_u - 1|k), 1) \leq \text{vec}(0)$$

$$G \text{vec}(\hat{z}(k + H_w|k), \dots, \hat{z}(k + H_p - 1|k), 1) \leq \text{vec}(0)$$

Here E, F and G are matrices of suitable dimensions depending on how many constraints we have in our optimization problem. For example, in our reservoir the inputs u can be the injection rates then, the matrix E would serve as a representative for the constraints on the actuator slew rates at the injection wells, the matrix F – for instance could be the

actuator ranges and the matrix G would be the representative for the constraints on our outputs which for instance is the BHPs at the injections wells.

The constraint equations thus take the form

$$E \begin{bmatrix} \Delta \mathbf{U}(\mathbf{k}) \\ \mathbf{I} \end{bmatrix} \leq 0; \quad F \begin{bmatrix} \mathbf{U}(\mathbf{k}) \\ \mathbf{I} \end{bmatrix} \leq 0; \quad G \begin{bmatrix} \mathbf{Z}(\mathbf{k}) \\ \mathbf{I} \end{bmatrix} \leq 0,$$

Here, the matrices $\Delta \mathbf{U}(\mathbf{k})$, $\mathbf{U}(\mathbf{k})$ and $\mathbf{Z}(\mathbf{k})$ are approximate functions of $\Delta \hat{u}$, \hat{u} and \hat{z} respectively.

All the constraint equation would also have to be written in terms of the optimization variable $\Delta \mathbf{U}(\mathbf{k})$ as

$$\begin{bmatrix} \mathcal{F} \\ \Gamma \\ \mathbf{W} \end{bmatrix} \Delta \mathbf{U}(\mathbf{k}) \leq \begin{bmatrix} -\mathcal{F}\mathbf{u}(k-1) - \mathbf{f} \\ -\Gamma[\Psi\mathbf{x}(k) + \Upsilon(\mathbf{u}(k-1))] - \mathbf{g} \\ \mathbf{w} \end{bmatrix}$$

For a detailed description of how the above equation was derived, the interested reader is advised to refer the detailed explanation provided on the MPC formulation as a quadratic programming covered in [21].

We would thus have our entire optimization problem as

$$\begin{aligned} & \min_{\Delta \mathbf{U}(\mathbf{k})} \{-V_k\} \\ & s. t. \quad \mathbf{A}_I \Delta \mathbf{U}(\mathbf{k}) \leq \mathbf{B}_I \end{aligned}$$

where

$$\mathbf{A}_I = \begin{bmatrix} \mathcal{F} \\ \Gamma \\ \mathbf{W} \end{bmatrix}; \quad \text{and} \quad \mathbf{B}_I = \begin{bmatrix} -\mathcal{F}\mathbf{u}(k-1) - \mathbf{f} \\ -\Gamma[\Psi\mathbf{x}(k) + \Upsilon(\mathbf{u}(k-1))] - \mathbf{g} \\ \mathbf{w} \end{bmatrix}$$

It should be noted that depending on the number of constraints and the number of grid blocks on our reservoir model, we could be dealing with dimensions of the matrices \mathbf{E} , \mathbf{F} and \mathbf{G} that are very large (say of the order of *no. of constraints* x *no. of grid blocks*)

unless we perform some kind of model order reduction. For this purpose we intend to reap the benefits of using a model identification method called System Identification which was dealt with in Section 4. Once we know our model and the constraints, the assembling of the matrices \mathbf{E} , \mathbf{F} and \mathbf{G} which appear in the standard formulation of the predictive control problem can be automated using either the *Model Predictive Control Toolbox* for *MATLAB*®, or by hard coding the procedure in an m-file sub procedure.

The proposed MPC controller for the production optimization problem would thus have an internal model generated by performing System-ID which would be used to predict the behavior of the reservoir, starting at the current time, over a future prediction horizon.

5.3 Operational Aspects

The flexibility of the constraints are obtained by using three weighing matrices, \mathbf{E} , \mathbf{F} and \mathbf{G} , with which the relative importance of respectively limiting the rate-of-change of the inputs, limiting the absolute value of the inputs and output target tracking can be adjusted. Apart from this, the two weights on the quadratic cost function (economic objective) namely \mathbf{Q} (penalizes deviations from the reference trajectory) and \mathbf{R} (penalizes change in the input vector) can be adjusted. The control and prediction horizons H_u and H_p , the weights on the constraints \mathbf{E} , \mathbf{F} and \mathbf{G} , the weights on the cost function \mathbf{Q} and \mathbf{R} , and the reference trajectory, all affect the behavior of the closed-loop reservoir model and the predictive controller. They need to be adjusted to give satisfactory dynamic performance. All these features together would definitely give the

production engineer total control over the behavior of the controller and hence the reservoir.

When implemented with the reduced state space matrices $(\mathbf{A}_r, \mathbf{B}_r, \mathbf{C}_r, \mathbf{D}_r)$, MPC has had important implications for its acceptance and development and computation speed thereby making it a good prospect for real-time control. Apart from freedom to adjust the formulation and the tuning parameters, it will allow production engineers to be relatively brave in introducing this new technology since if he wants to temporarily inactivate the controller, it is usually possible to disable it and let the local loop controllers hold the reservoir simulator at the last set-points they received from higher levels. It is also very much possible for the integration of economic short-term set-point optimization with the dynamic performance optimization strategy formulated and implemented in the model predictive controller. The reader can refer to publications on the use of reduced order models in control and optimization [11] [13].

6. MPC AND SYSTEM-ID – CASE STUDIES AND CONCLUSIONS

In this Section we will be focusing on the combined performance of Model Predictive Control and System-ID for two cases in particular. Some important discussion would be about the identification of the system around various critical work points and the decision and logics that were made in the design stage of the MPC controller. As we know by now that designing the proper MPC framework after identifying the model is one of the most important and time consuming task. The level of detail in coming up with our optimization problem as well as the quality of the model at each stage of the control process have a direct effect on the effectiveness of the waterflooding process.

6.1 Case 1 – The Five Spot 2D Reservoir

The reservoir model that we would be dealing with is almost the same as the one that was used as the toy model for evaluating the performance of system identification in the previous Section. The reservoir has four production wells at the four corners and a water injector at the center as shown in Figure 6-1. The total number of inputs that can be manipulated are five. This includes the bottom hole pressures (BHP's) of the four producers and the water injection rate of the well placed at the center. The Table 6-1 shows the reservoir and fluid properties that were considered for this case.

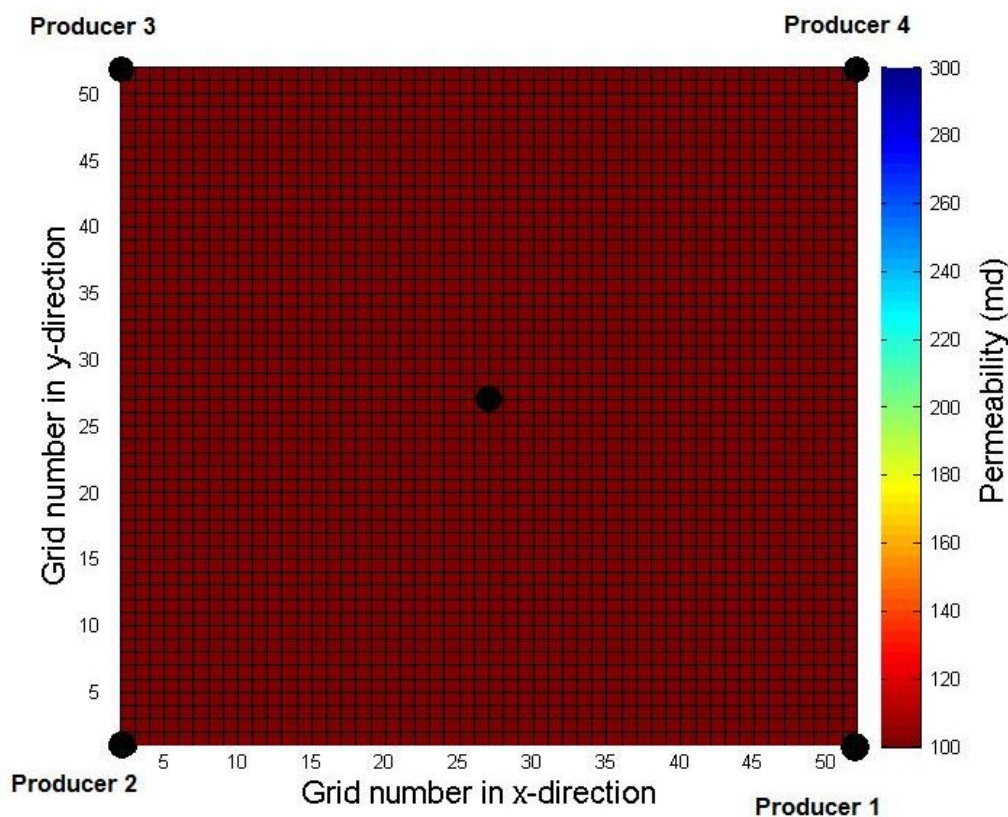


Figure 6-1 Homogeneous Reservoir for Case 1

Table 6-1 Reservoir and Fluid Properties for Case 1

Variable	Description	Value	Unit
ρ_o	Density of Oil	45.0	lbm/ft ³
ρ_w	Density of Water	62.0	lbm/ft ³
μ_o	Viscosity of Oil	10	cp
μ_w	Viscosity of Water	.89	cp
c_o	Compressibility of Oil	10×10^{-6}	psi ⁻¹
P_o	Initial Pressure	3800	psia
S_o	Initial Saturation	0.1	[-]
ϕ	Rock Porosity	.20	[-]

The Figure 6-2 presents the production rates for the homogenous case reservoir assuming that it is to be produced for a period of 1400 days. The reservoir was

optimized in an open-loop fashion by using the *fmincon* optimization function in Matlab®. This is a gradient-based optimization procedure as was described in Section 2. The reservoir was optimized just once at the beginning for the entire life cycle of the reservoir which is for 1400 days. The reason why 1400 days was decided as the end of the production life was because by that time the watercut at the production had exceeded a set value (for our case it was set at 90%). The oil price for the optimization problem was assumed to be fixed at \$85 per barrel and the separation cost of water at the production well was assumed to be at \$1 per Barrel. It was also assumed that the cost to injecting water is zero.

Since the reservoir is homogenous and has a perfect symmetry from the injection well at the center to the production wells at the four corners of the reservoir, the optimization using *fmincon* would obviously result in a single constant injection rate that would be followed throughout the life of the reservoir. The objective function was to maximize the net present value which was a function of the oil production rate, water production rate, cost of oil per barrel, and cost of water separation per barrel.

As expected, the trajectory for all the wells are the same due to geometric symmetry and homogeneity. The optimized injection rate of 8000 bbl/day was applied for the life of the reservoir and the Production BHPs were maintained at 5800 psi. Since this was a pretty straight forward case, the time step at 20 days was enough to capture the dynamics and hence was decided as the sampling time.

The water front reached the production wells at 1186 days. The reservoir was run till the water cut reached 60%. The profit calculated by the NPV was at \$ 65.3 million at the end of 1400 days.

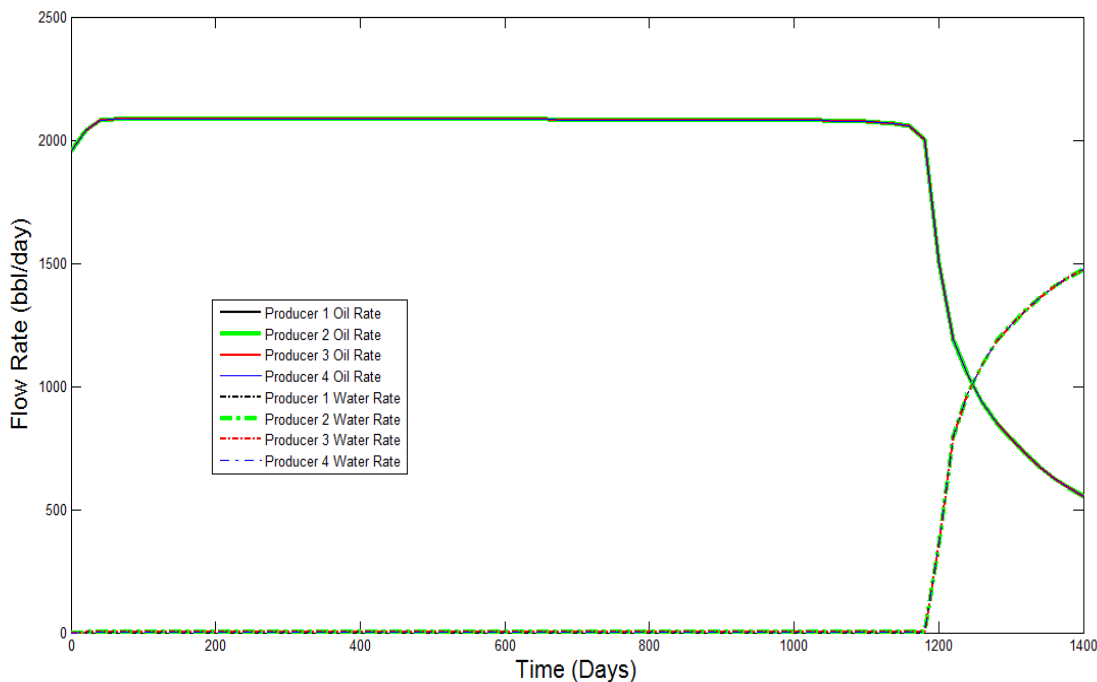


Figure 6-2 Phase Rates for Homogeneous Reservoir

The next step is to introduce a channel of high permeability region between producer number two and the injection well as shown in figure. In a real reservoir there would be regions of high and low permeabilities. Our purpose of introducing the high permeability region is to analyse the performance of MPC in a heterogeneous reservoir. There is a natural tendency in the reservoir to produce at a higher rate from the high

permeability region. This would in turn effect in a much earlier water break through in well number two to which the liquid from high permeable region flows.

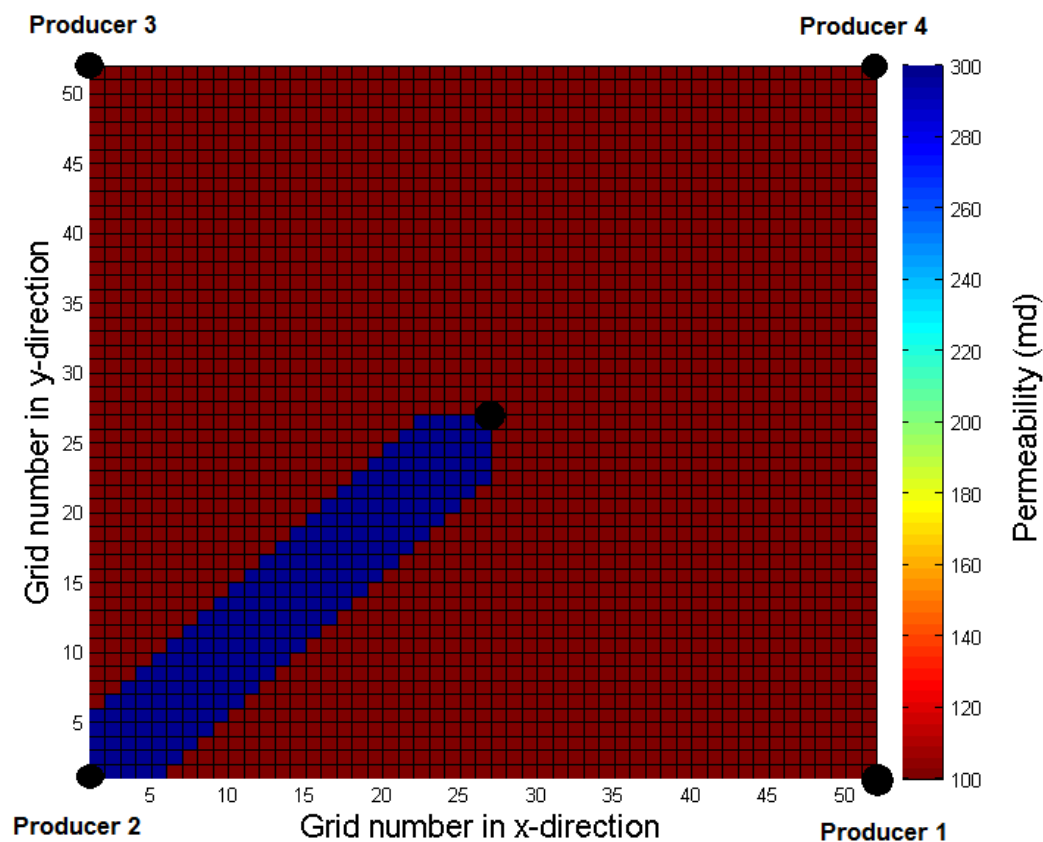


Figure 6-3 Homogeneous Reservoir with High-Perm Channel for Case 1

For our present scenario, by introducing a high permeable region (as shown in Figure 6-3) towards the direction of well number two, we would expect an increase in the production for that well and water cut at a much earlier time. The high perm channel has a permeability that is three times higher than that for the rest of the reservoir as shown in the color bar.

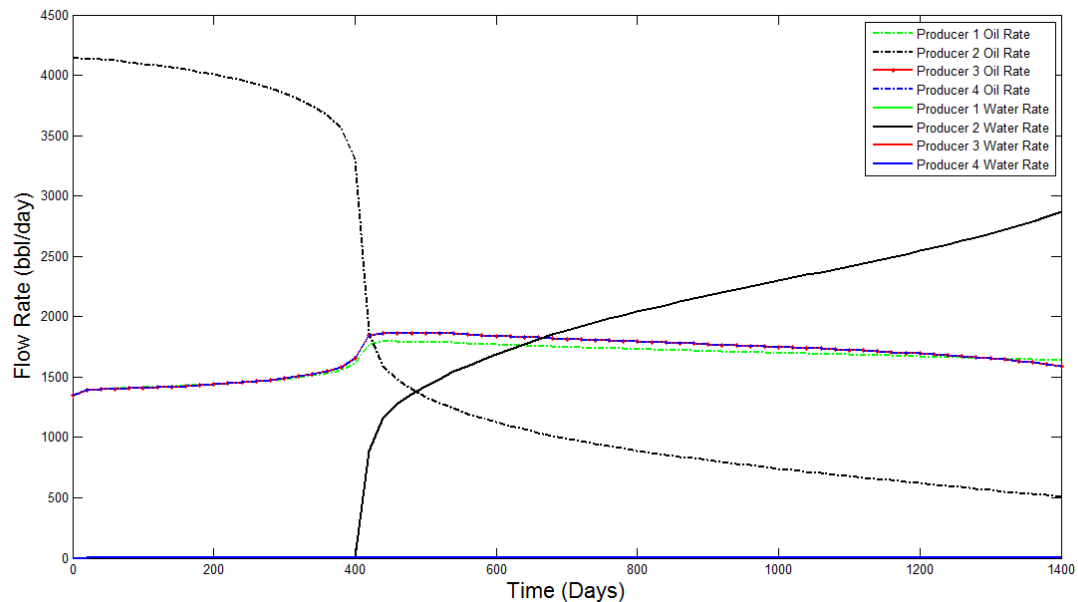


Figure 6-4 Open-loop Phase Rates for Homogeneous Reservoir with Channel

As we would expect, the oil production of well number two is significantly higher than the rest of the wells. This can be seen in Figure 6-4. The production rate at well number two is higher than the maximum production rate in the homogeneous case whereas for the rest of the wells, it is lower. Consequently, the producer number two produces water at a much earlier date. It starts producing at about 400 days compared to about 1200 days for the homogeneous case. The calculated profit for this case was \$ 53.3 million which is about 18.3% less than the value for the homogenous case.

6.1.1 Performance Enhancement Using MPC

The open- loop optimized control for both the homogeneous and heterogenous reservoir was created and compared with the intention to evaluate the performance of our MPC in dealing with a heterogenous reservoir. We could witness a significant decrease in NPV and a much earlier water cut for the reservoir with the high perm channel. It would have been better if we could somehow prevent this from happening. What we would ideally want is that the water front still approach all the production wells at the same time so that - when the production rate of water at the wells would have reached uneconomic levels, we would have already depleted the reservoir somewhat uniformly and completely, thereby ensuring a higher NPV.

With this idea in mind we aim to follow production trajectories for the homogeneous case eventhough the reservoir is now heterogenous. The reference trajectory for MPC was thus set as shown in Figure 6-2.

The next step is to integrate the MPC control algorithm with the identified model. Our aim is to optimize the control inputs (which in this case is the water injection flow rates and the Production BHPs at the four wells) for a period of time (the life time of the reservoir), such that the outputs (Production Rates) would be steered to the optimal trajectories found for the homogenous case, thereby ensuring a significantly higher NPV and delayed Water break through.

6.1.2 The Identification

First, a model was identified. The subspace identification scheme as suggested by above was applied to the Eclipse® model data in order to identify a state space model. The identification routine was written in Matlab®, using the subspace identification function (*SUBID*) by Van overschee and De Moor available at the website of the Department of Electrical Engineering, Katholieke Universiteit Leuven [17]. The input to the system is the water injection rate and the production BHPs. The outputs available were the BHPs of the four wells and the water injection BHP. This supplies us with the following vectors.

$$\begin{aligned}
 u_k &= (bhp_k^{P1} \quad bhp_k^{P2} \quad bhp_k^{P3} \quad bhp_k^{P4} \quad q_k^{I1})^T \\
 y_k^p &= (q_k^{P1} \quad q_k^{P2} \quad q_k^{P3} \quad q_k^{P4} \quad bhp_k^{I1})^T \\
 y_k^l &= (opr_k^{P1} \quad opr_k^{P2} \quad opr_k^{P3} \quad opr_k^{P4} \quad wpr_k^{P1} \quad wpr_k^{P2} \quad wpr_k^{P3} \quad wpr_k^{P4})^T \\
 y_k &= \begin{pmatrix} y_k^p \\ y_k^l \end{pmatrix}
 \end{aligned}$$

Figure 6-5 presents the simulation fit of one of the outputs (producer one oil rate). In the early stage of waterflooding before the production wells have felt the waterfront, the reservoir has a somewhat simple underlying dynamics. For this reason, as could be seen from the graph, a good simulation match was obtained.

Performing subspace identification with order 6 . It need to be noted that we are performing subspace identification on an reservoir simulator model with grid cells 51 x 51. The full order model is of size 5202 x 5202. This is a measure of the size of the state space input matrix if no reduction is performed. That would mean that we are dealing

with a system of order 5202. The order of the identified model is only 6. Thus there is a significant decrease in computational effort when using an identified model instead of the actual reservoir model. Moreover, the identified model could also give a simulation fit of 97% for this case.

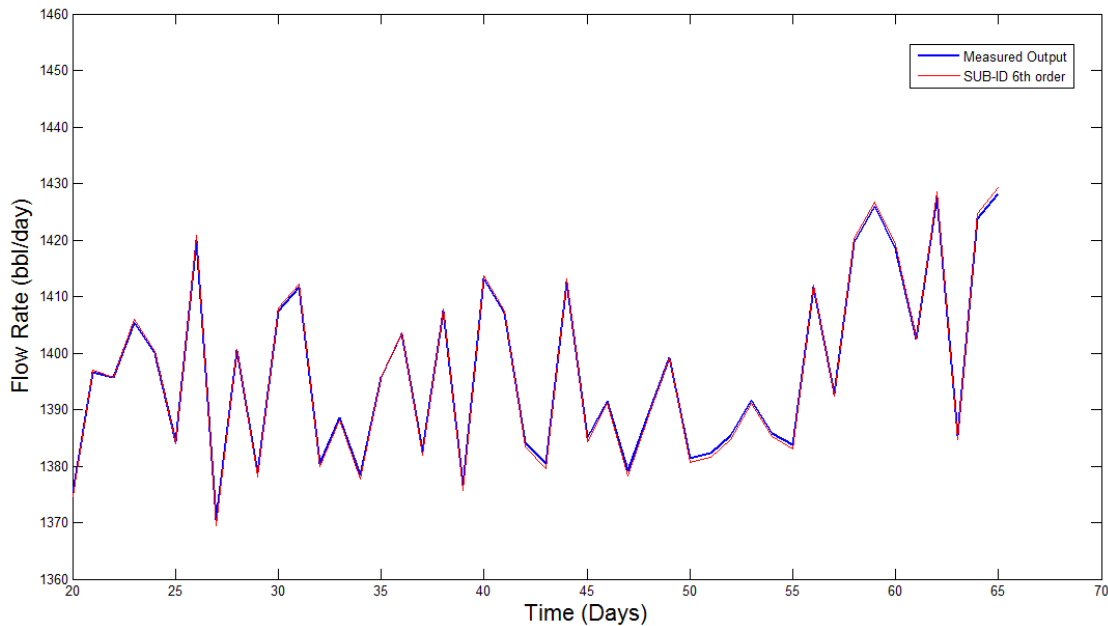


Figure 6-5 Simulation Fit for Homogeneous Reservoir with Channel

The identification was carried out by generating random input signals for 65 days. We know for a fact that the optimal input signal is going to be somewhat constant for a significant period in the early stages of the reservoir (less than 200 days) as could be seen in the homogenous case discussed earlier. (This is because the water front has not yet reached the reservoir boundaries. Such a signal cannot be applied as inputs while performing system identification because the “constant” input signals will not be able to excite the system dynamics and therefore we would not be able to get important

information about the system. Thus the random variation in input is added on top of the inputs.

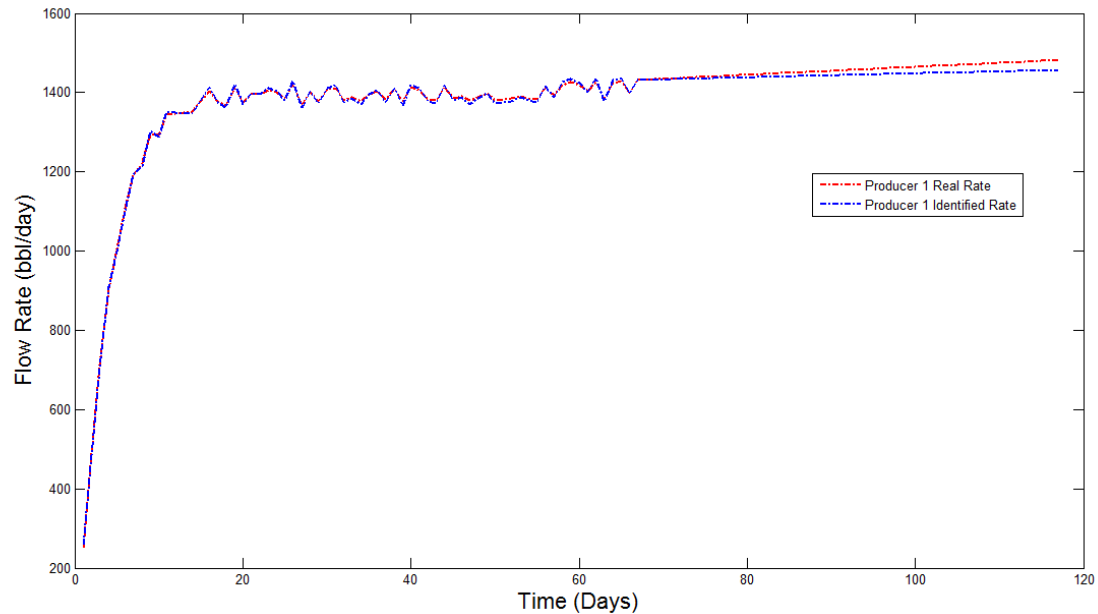


Figure 6-6 Expanded Simulation Fit for Homogeneous Reservoir with Channel

The Figure 6-6 shows the prediction quality of the identified model. Eventhough System-ID was performed only for 65 days, the identified model predicts the ‘real-model’ somewhat accurately for to upto 120 days. In the period beyond 65 days, we were able to achieve a simulation fit of 81% which is quite surprising. An interesting observation to note is that the identified model could also predict the slight increase in the production flow rate which occurs clearly after the period for which subspace identification was performed. Similar to this, subsequent decrease or increase in

production was also observed for the identified models of well two, three and four quite effectively till 120 days.

6.1.3 Results before Water Breakthrough

Figure 6-7 presents the primary results obtained while optimising the inputs through predictive control. The control action is initially triggered when the production wells sense a reasonable increase in the water production rate. For the current case, we could notice that the trigger occurs at around 70 days. This is because there has been an increase in the water production rate at the well number two (which is situated at the high permeability corner in the reservoir). The control action therefore suggests to increase the BHP for that particular well and decrease the BHP for the remaining wells. This is shown in Figure 6-7 as we can notice an increase in the BHP of well number two to 5805 psi whereas a decrease in the BHP of the remaining wells to about 5735 BHP.

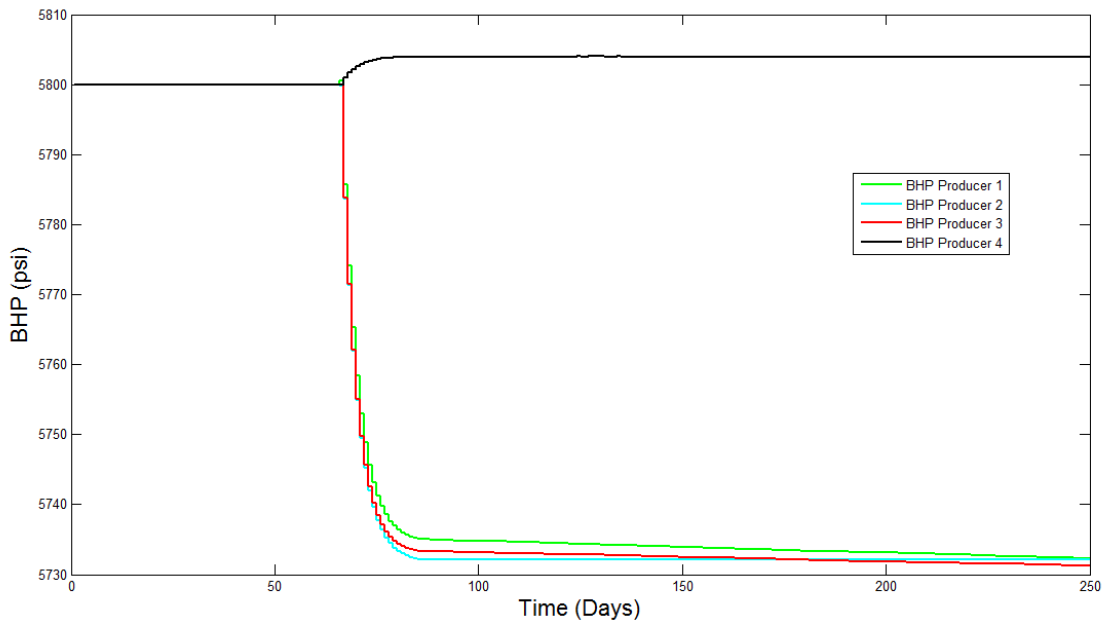


Figure 6-7 MPC Input-BHP for Homogeneous Reservoir with Channel

This change in BHP would inturn effect flow rate to decrease its value in well number two and to increase its value for the remaining wells. As shown in Figure 6-8 we can see that the production rates for all the wells tends to reach its reference trajectory – which is the optimal trajectory as computed in the previous case shown as the blue line at about 2010 bbl/day. Even though all the production flow rate are supposed to be maintained at the optimal value throughout the life of the reservoir, this is not what ideally happens in our case.

We could see that there is a significant deviation for the flow rate in well number two. It infact decreases way below the 2010 bbl/day line at about 250 days. This is accounted for, by the decease in prediction quality for the identified model as shown in Figure 6-8. The prediction curve suggests by about 120 days into production, we have

already lost the simulation fit by about 20%. This would obviously suggest a significant decrease in prediction quality at 250 days into production when we use the same single model as identified at the initial stage of our reservoir. The model could probably not recognise the increase in water production especially in well number two as a result of the progression of the water front through the high-perm channel.

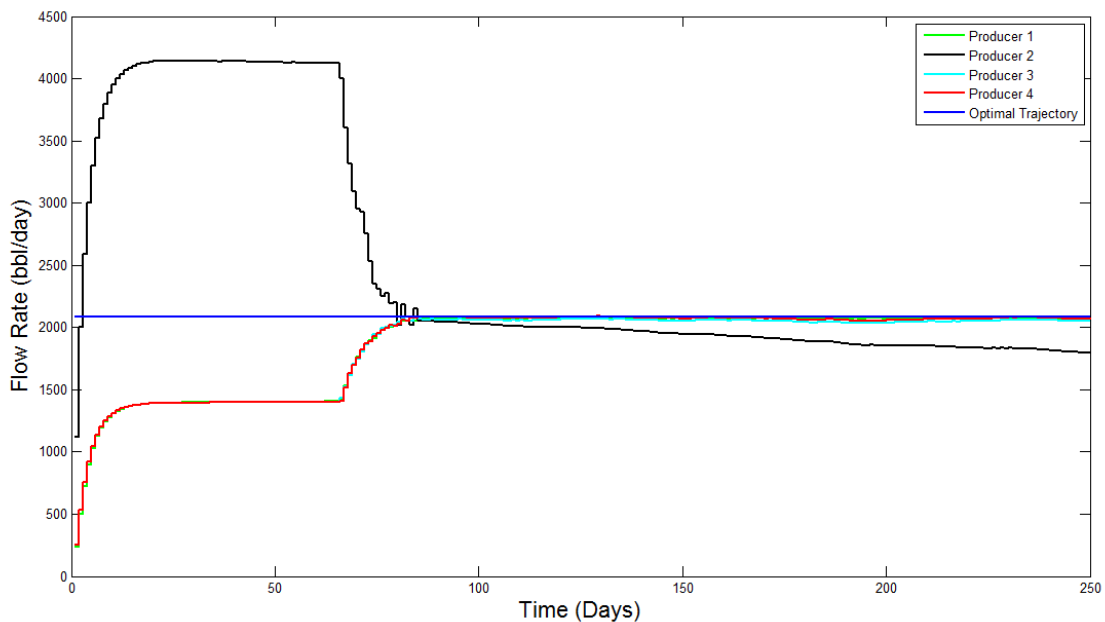


Figure 6-8 MPC Outputs for Homogeneous Reservoir with Channel

Figure 6-9 shows the MPC optimized injection rates that was used to generate the outputs in Figure 6-8. It could be seen that there is a steep decrease in the injection rate once the water production rates to rise in the wells. The exponential-like curves in Figure 6-8 and Figure 6-9 are as a result of limiting the input variations in the time steps. Beyond 70 days we can notice slight dynamic variations in the injection rates and BHPs of the production wells because of the tight control in the inputs. Neither the injection

rates nor the production BHPs have changed noticeably. The output behavior for this period of the life cycle of the reservoir can be interpreted by the fact that - by the time we pass 70 days, the inputs become somewhat steady and reaches the same value in all the wells and hence, force the outputs to be as close to the optimal trajectories as possible.

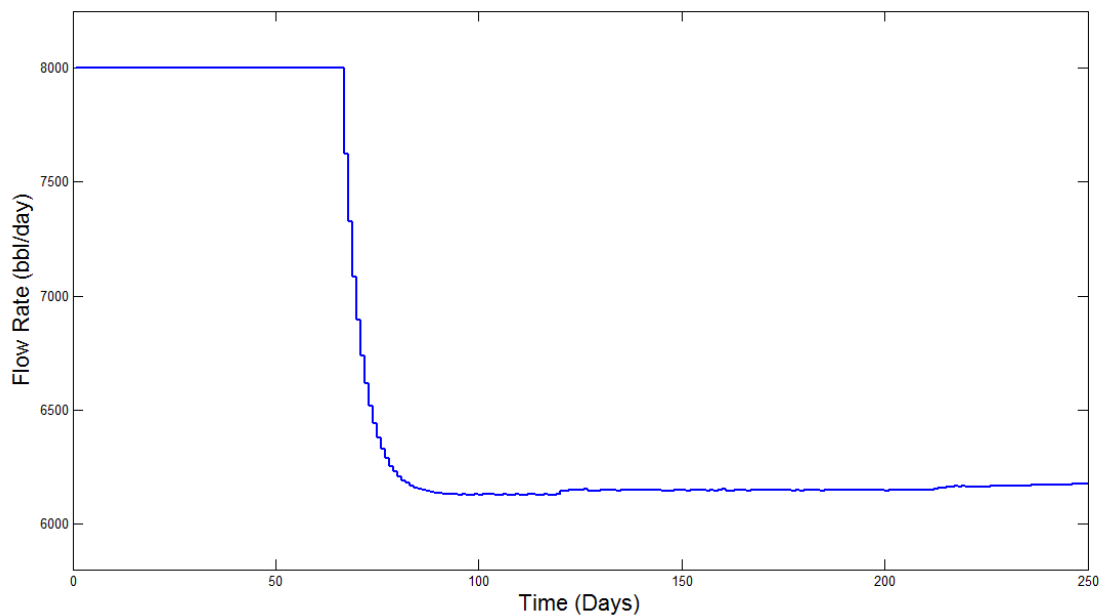


Figure 6-9 MPC Input-Rates for Homogeneous Reservoir with Channel

6.1.4 The Big Picture

This Section concludes the result obtained by performing the closed-loop control for the complete life of the reservoir. As was decided previously, our motivation in using this reservoir was to evaluate the control algorithm of MPC in driving the outputs dynamically toward its set reference trajectories. This is quite successful as we could see in Figure 6-10. Taking this methodology a step further, we then wished to see the results

obtained after water breakthrough. The end of the life of the reservoir for our simulation experiment was decided as 100 days after water breakthrough because by that time we can capture important dynamics of the reservoir without compromising on the validity of the identified model.

Care needed to be taken to ensure that we updated the model atleast once before we could use the model for MPC because we have already noticed a significant drop in prediction quality by 250 days into production. Though this is the case, we decided to use the same model till about 600 days because by then the water front could sense atleast one of the wells.

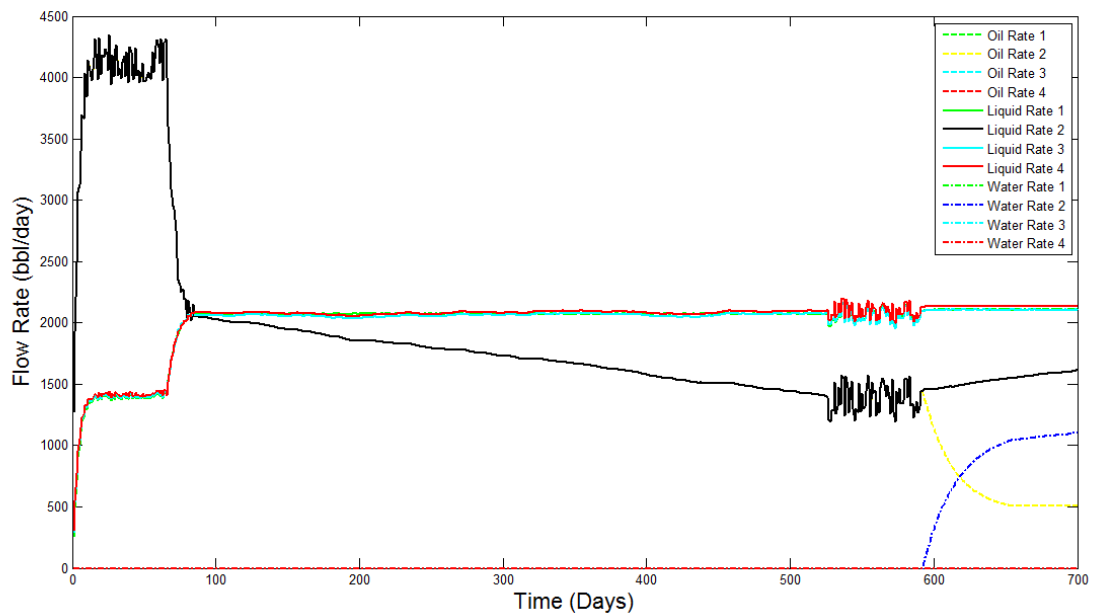


Figure 6-10 MPC Optimized Lifecycle Production Phase Rates – Case 1

6.1.4.1 The Expanded Model

At the end of this period, a new model had to be identified. For the purpose of identification, the random input signals were imposed upon the last 65 days of production data. The resulting flow rates (outputs) could be seen as the second random period in the figure above. The random signal used to perform this identification has the same properties as the signal used for the first case though the state of randomness is different.

However the same number of inputs and outputs could not be used for this identification because we need to account for the additional dynamics that occur due to water breakthrough. The presence of water at the producing well contributes to the pressure dynamics and makes them nonlinear. Thus, in order to represent this case, the identification process has to be embedded with the amount of water that has broken through. This is taken care of by augmenting the number of outputs used by including the WOR (Water-Oil Ratio) in the form of water production rate and oil production rate for performing system identification.

Thus the total number of inputs would still remain the same at five (i.e. one injection well rate and four production well BHPs) and the total number of outputs is augmented to eight (i.e. the four water production rates and the four oil production rates at the four wells). This identified Model does not really do a very good job when compared to the identification we were able to make for the period before the Water breakthrough as was shown in the history matching plot in Figure 6-10.

6.1.4.2 Production Prediction after Water Breakthrough

As presented in Figure 6-10, we could notice that the liquid rate in well number two, which dropped way below the optimal rate settings set as per the homogeneous model, is now catching up with the optimal reference trajectory as a result of performing the second identification. It would have definitely been better if we could perform identification at intermediary stages so that we wouldn't lose the model quality. This decision need to be made after conducting numerous simulation experiments with system identification conducted at different intervals for each case. In this manner, we can come up with the most beneficial waterflooding control strategy.

Our closed-loop control performance by identifying the system twice has resulted in a significant improvement in the NPV. We were able to achieve a profit of \$31.32 million when this reservoir was optimized for 700 days compared to a profit of \$ 25.61 million when optimized in an open loop fashion for the same period of time. In addition to this, we were also able to delay the water breakthrough by about 195 days.

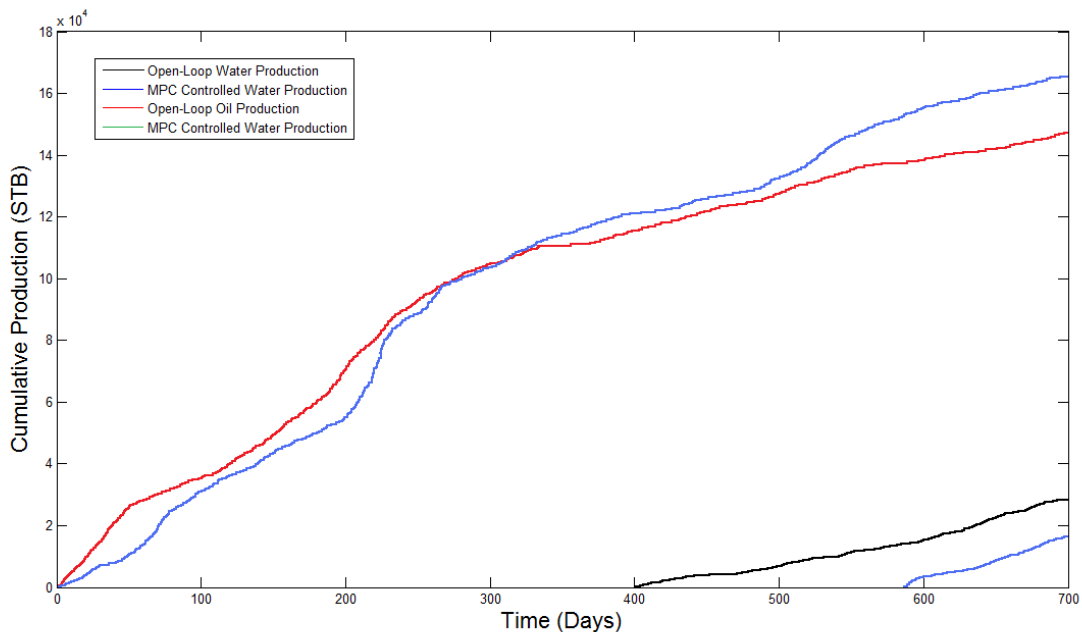


Figure 6-11 MPC Optimized Lifecycle Cumulative Production – Case 1

The Figure 6-11 shows the cumulative production trajectories of oil and water for both the open-loop and closed-loop case. We could see that after about 300 days into production, the MPC controlled overtook the open-loop optimized reservoir in cumulative oil production. At the end of the 700 days period, we could also notice a significant improvement in the cumulative oil production. In addition to this, by performing optimization using MPC and System-ID, we were also able to delay the water production by about 190 days.

6.2 Case 2 – A Fine Grid Geostatistically Generated Field

The 10th SPE comparative solutions project presented a model that could be used to study Black-oil, compositional, dual porosity, thermal or miscible simulations, as well as horizontal wells and gridding techniques. Our purpose of using this comparative solutions project was to evaluate the effectiveness of system identification. The task performed by upscaling and other pseudoization methods in the comparative solutions project was similar to what system identification would have to perform in our case, as both aims at reducing the size of the reservoir model. We had to evaluate its performance on a 1.1 million cell geostatistical model that would be used to study waterflooding. The size of the model makes the use of classical pseudoization methods or having a full fine grid solution impractical.

6.2.1 Reservoir Model Description

The model used for SPE 10 was originally generated for use in the PUNQ project¹⁵. The model consists of part of a Brent sequence. The vertical permeability of the model used for SPE 10 was altered from the original (i.e. PUNQ): originally the model had a uniform k_v/k_h across the whole domain. The model used here has a k_v/k_h of 0.3 in the channels, and a k_v/k_h of 10^{-3} in the background. The top part of the model is a Tarbert formation, and is a representation of a prograding near shore environment. The lower part (Upper Ness) is fluvial.

The reservoir model presented (Figure 6-12) for the SPE 10 comparative project has a simple geometry, with no top structure or faults. The reason why this was provided

was to provide maximum flexibility in the selection of the upscaled grids that could be tested on the model. At the fine geological model scale, the model is described on a regular cartesian grid. The model dimensions are 1200 x 2200 x 170 (ft). The top 70 ft (35 layers) represents the Tarbert formation, and the bottom 100 ft (50 layers) represents Upper Ness. The fine scale cell size is 20 ft x 10 ft x 2 ft. The fine scale model has 60 x 220 x 85 cells (1.122x10⁶ cells).

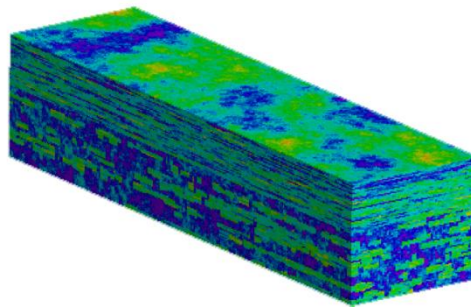


Figure 6-12 Reservoir Model for Case 2

The top slice of the reservoir was used for our study as we are dealing with the 2-D reservoir model. Thus we would be dealing with a model of size 60 x 220. The reservoir and fluid properties are shown in Table 6-2.

6.2.2 Well Placement

The porosity and permeability distribution is shown in Figure 6-13. We could notice that the reservoir has flow channels directed in the top – bottom direction rather than in the left – right direction. So according to the reservoir engineering basic fundamentals, we would want to place injectors and producers in such a way that

injector- producer direction does not align with the reservoir's flow channels. Thus the water injected would have to go across the flow channels than through the flow channels, thus ensuring that the injected water could effectively displace the oil and hence we would expect the water cut to occur at a later time only once the oil has been somewhat completely displaced.

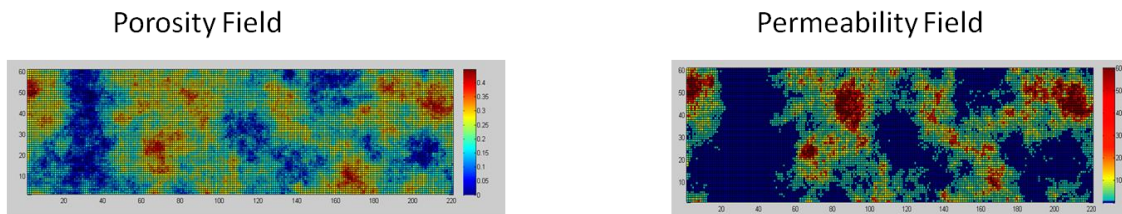


Figure 6-13 Porosity and Permeability Field for Case 2

With this idea in mind we would place the injector and producer in the left – right direction (i.e. – the injectors at the right side and producers at the left side, or vice versa). For our case we placed five equally spaced injectors at the right side and five equally spaced producers at the left side. Even though this line-up of injectors and producers would be beneficial for waterflooding, it would not pose as a good problem to discuss or to interpret the effectiveness of waterflooding using our MPC and System-ID approach.

Table 6-2 Reservoir and Fluid Properties for Case 2

Variable	Description	Value	Unit
ρ_o	Density of Oil	45.0	lbm/ft ³
ρ_w	Density of Water	62.0	lbm/ft ³
μ_o	Viscosity of Oil	10	cp
μ_w	Viscosity of Water	.89	cp
c_o	Compressibility of Oil	10×10^{-6}	psi ⁻¹
P_o	Initial Pressure	3000	psia
S_o	Initial Saturation	0.1	[-]
ϕ	Rock Porosity	.20	[-]

In other words, by placing our injectors and produces in the top – down direction, even though we would expect a water-cut at an earlier time, we could clearly evaluate the performance of MPC and System-ID in bringing out an effective waterflooding for the reservoir. In summary, the reasons for our injector – producer placements are:

- To pose a good problem wherein the well placement is not ideal for waterflooding the reservoir.
- To deal with a reservoir whose tendency to produce water in some of the production wells is much faster than the remaining production wells. (Since the flow channels are aligned in the same direction as the Injection- Production well direction.
- Placing wells in the left-right direction has an obvious disadvantage of having to perform System identification for more number of times as opposed to when waterflooding in the top – down direction. This is primarily because the change in reservoir dynamics is much more prominent since a longer time is required for wells and the flow would have to be through much more prominent variation of

permeability or porosity. Thus to interpret the results and effectiveness, it's enough to deplete the reservoir within a shorter span of time, as similar good results can be obtained if we wish to place wells in the left-right direction.

The system identification was performed in the same manner as explained in the Section 4. The knowledge obtained by performing the step response and staircase experiment were the judgmental in coming up with the appropriate design of the input signal. The length of the input signal required for identification was decided based upon the type of reservoir at hand and the purpose of identification.

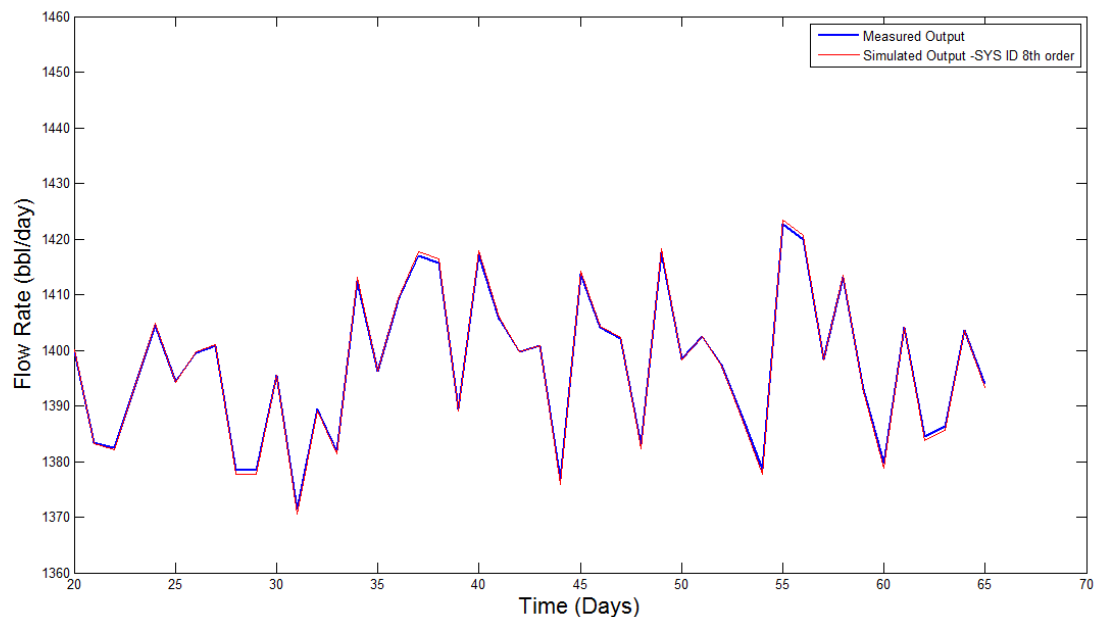


Figure 6-14 Simulation Fit for Case 2

The Figure 6-14 shows the simulation fit of the identified model. Due to the simple underlying dynamics in the earlier stage of the reservoir, we can see that a very

good simulation fit can be reached with lower order models. In the period between 20 and 65 days, the model output and the reality measured values are very close (more than 97% fit) as it is the same period for identification. Identifying lower order models was possible but we had to make a trade-off between the accuracy to predict the output closely enough until the next System-ID is performed and computational effort. A good observation was the ability of the model to predict the output accurately enough for the next 80 days, (90% fit).

For periods 30-70 and 70-150 the reference tracking quality is better, but needs to be noted that for the last period the prediction quality is not good enough. This is obvious because of the fact that MPC controller doesn't perform well due to the nonlinearity effects of water breakthrough. This is an indication for us that it is time to perform model identification. Since water breakthrough has occurred, we can take into consideration a new parameter - oil-water ratios at the production wells while performing system identification. So the total number of inputs would be five (i.e. the five BHPs at the production wells) and the total number of outputs would be ten (i.e. the five production rates and the five water-oil ratios at the production wells).

6.2.3 Model Dynamics

One of the biggest challenges was to come up with an identified model. Analyzing all the input and output pairs from the 5 different wells one by one seemed like a very time consuming task since in each pair, both the step response as well as the stair case experiment had to be interpreted simultaneously to design the best input signal

that could serve and predict the outputs effectively for each of the five pair of wells. Another issue is the number of inputs and outputs we wish to control and predict respectively. For this model we assumed that the injector rates are already fixed to their optimal value as computed from the performing the open loop optimization. By this step we reduced the number of controllable inputs from ten inputs to five since we are only interested in manipulating the BHP for the producers. This would definitely make the problem formulation easier from the system identification point of view as by reducing the number of inputs we have compromised on the degrees of freedom for the MPC controller. This is another trade-off that needs to be made.

6.2.4 MPC Implementation

The Figure 6-15 below presents the reservoir production flow rates during the life of the reservoir at producer number five. Also included in the same figure is the uncontrolled production rate which is presented with the intension to point out the benefits and specific advantages of using the MPC controller. The random variation of the outputs (flow rates of producer one) at four instances is shown explicitly in this graph so that we can observe the time intervals at which model identification has been carried out.

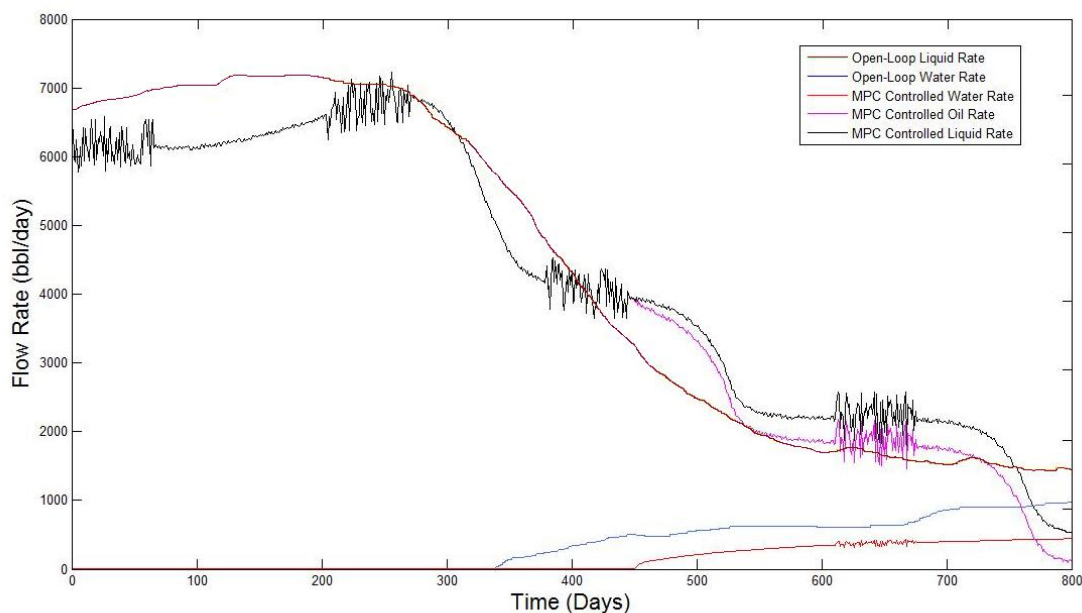


Figure 6-15 MPC Optimized Open-Loop and Closed-Loop Phase Rates – Well 5

The random input signals that were generated to perform system identification were also used in the reservoir model. This would not be required when the actual MPC control algorithm needs to be implemented in the real reservoir. This is to say that the input signal used for model identification would not be used while performing the closed loop optimization in the actual reservoir but instead, the optimal inputs as computed by the MPC control algorithm will be used.

Looking at the Figure 6-15, we can also see that the production rates at the earlier stage in the life cycle of the reservoir are higher for the open-loop controller when compared with that obtained by using the closed-loop MPC controller. Though this is the case, at the later stages, it could be noted that by using the MPC controller there is noticeable improvement in the production rate at well number five. Looking back at the

location of well number five in Figure 6-13 we can see that the well is located near a permeable region, which is the reason why there is reasonably high production rates in the earlier stages of the reservoir be it in open-loop or closed-loop control.

As time progresses till about 750 days, though the production well has a natural tendency to have a reduction in the total liquid production rates, the MPC controller limits this decrease. Therefore, it will have lower production rates unless it is controlled with updated inputs. Apart from steering the total liquid production rate to a higher level the Water production rates are also lower due to the MPC control. Looking at the water production rates, it could be notes that there is a good delay in the water break through that is obtained as a result of our closed-loop control of the production BHPs. Water production for the producer well number five starts at about 340 days for the open-loop controlled case whereas it only starts at around 450 days by MPC.

Similar results are obtained at producers one, two, three and four as shown in Figure 6-16, Figure 6-17 Figure 6-18 and Figure 6-19 respectively. We could notice that if water production rates at all these wells are lower when compared to the open-loop case especially at the end of the 700 days. Apart from that, there is a significant improvement in the oil production rates too.

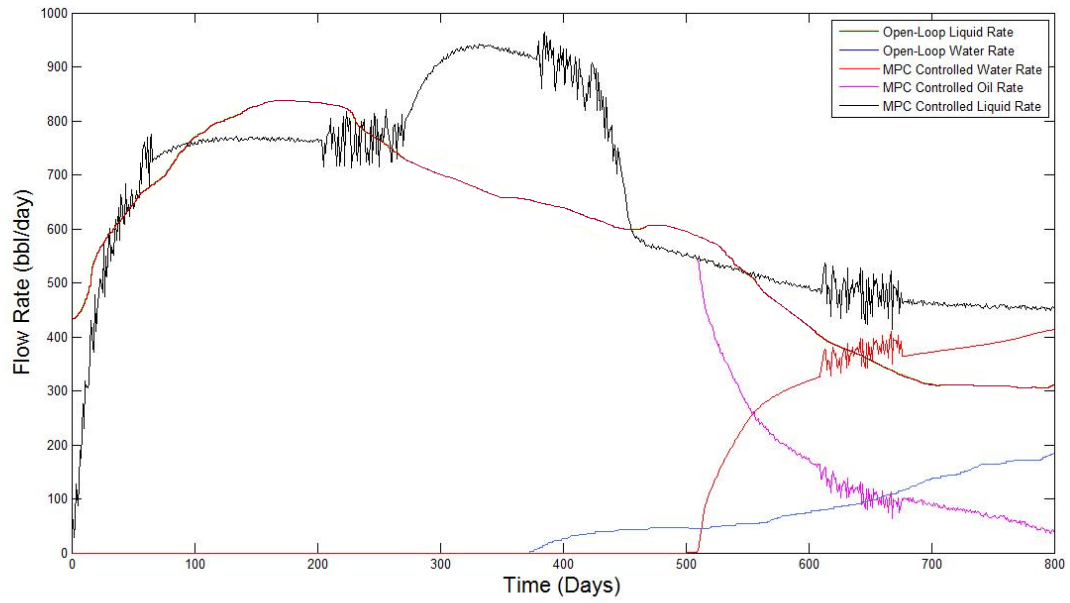


Figure 6-16 MPC Optimized Open-Loop and Closed-Loop Phase Rates – Well 1

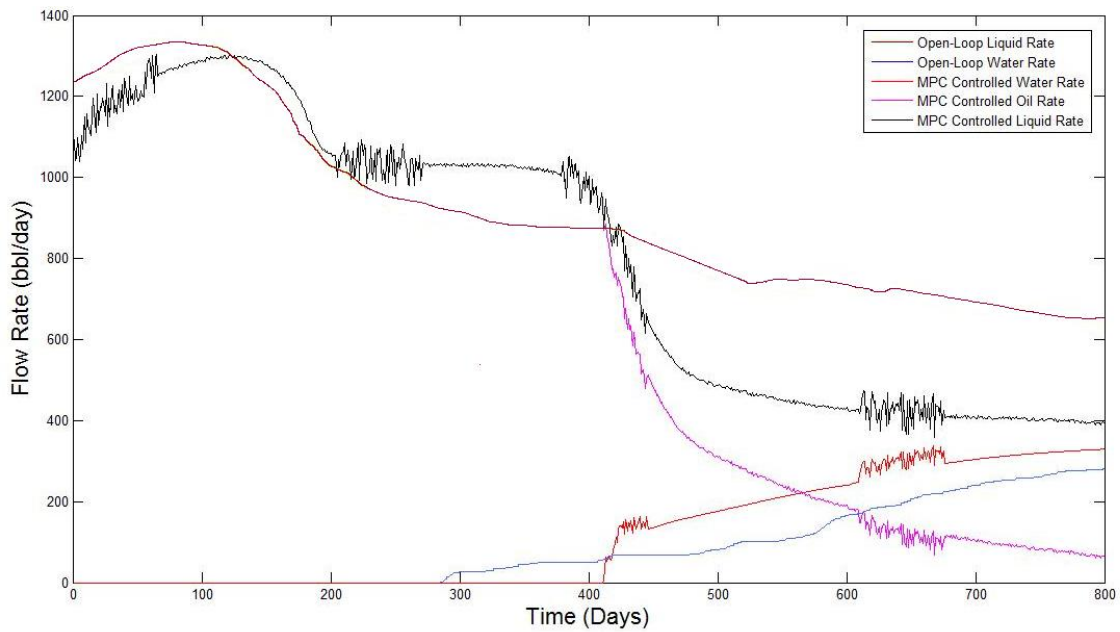


Figure 6-17 MPC Optimized Open-Loop and Closed-Loop Phase Rates – Well 2

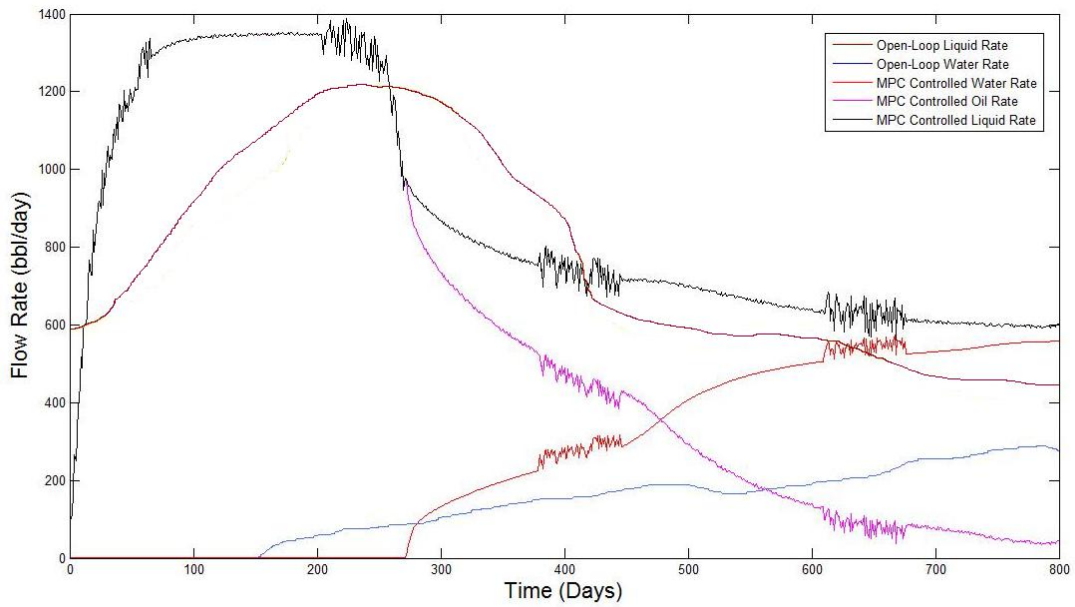


Figure 6-18 MPC Optimized Open-Loop and Closed-Loop Phase Rates – Well 3

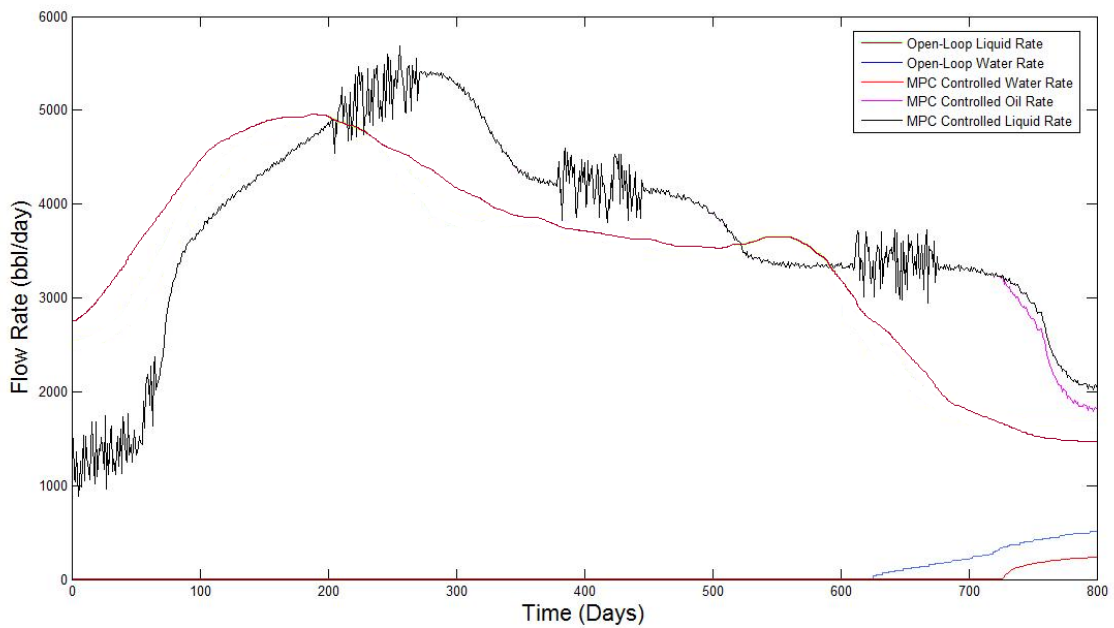


Figure 6-19 MPC Optimized Open-Loop and Closed-Loop Phase Rates – Well 4

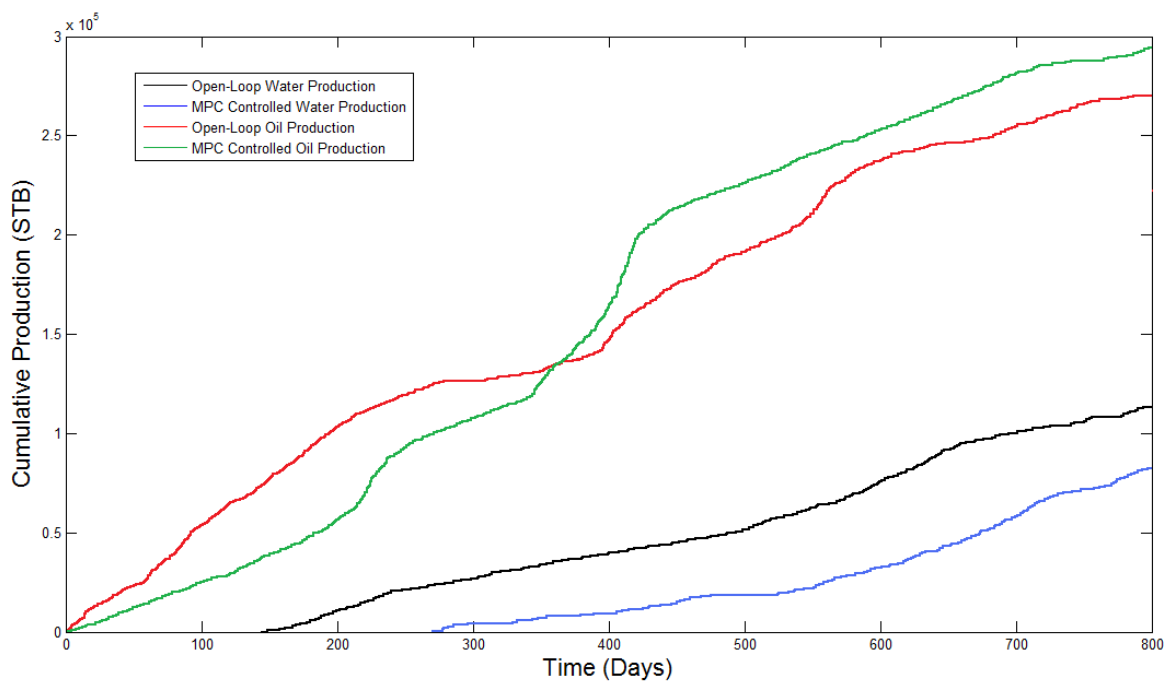


Figure 6-20 MPC Optimized Lifecycle Cumulative Production - Case 2

The cumulative production graph shown in Figure 6-20 is a good indicator to validate the improvement in optimization and ultimate oil recovery as far as our closed-loop control is concerned. We could notice that even though the cumulative oil production was higher for the open-loop case in the early production phase of the reservoir (till about 360 days), beyond this time we can observe a significant improvement in production by implementing the MPC controller.

6.3 Conclusions

This paper presented a general framework for realizing real-time optimal control strategies for large-scale reservoir models. As it is the case of most of oil reservoir

models, uncertainty in the geological and petrophysical parameters are the main drawbacks of open-loop optimization. After observing the improvements in oil recovery and reductions in water production effectively for both the cases that were considered, we can reinforce our stance in proposing the implementation of MPC and System-ID towards the ultimate goal of “real time” production optimization. In addition to obtaining a significant reduction in computational effort without compromising on model quality or control objectives, we were also able to provide a much more robust control together with excellent constraint handling capabilities.

Closed-loop control has the potential to address issues related to production optimization given a set of unknown parameters as in any other engineering discipline taking advantage of real-time data management. However, the size of the models due to the discretization of the partial differential equations are very large (as compared with other disciplines) and are not amenable for fast implementations, or may require large amount of computational power.

Solution techniques that involve efficient numerical computations for parameter estimation and optimization are of great value in these settings. Model reduction techniques may be the only way to avoid the large scale computations that takes place in the optimization process. It is fair to say that closed-loop reservoir management is still in its infancy and much attention and resources need to be put forth for realizing its full potential.

6.4 Research Gaps

Basically, the concept of closed-loop reservoir management has been shown to be of great value in the literature, but the introduction of such methodologies has not been fully accepted (or it has a slow pace) in practical applications in the Oil & Gas industry. The main issues are fourfold:

1. Though great improvements in control capabilities have been observed in this research, the nonlinearities of the reservoir as such have not been dealt with in this research. This is an important area that is still an open topic to be researched on. The highly nonlinear behavior of reservoir models could be dealt with by the use of nonlinear schemes like Nonlinear Model Predictive Control (NMPC). The experiments conducted on system identification in my research suggests that when identification is performed for more times, the better I could account for that otherwise unavailable knowledge of the important dynamics taking place in the reservoir. This requirement can be surpassed to a great extent by implementing NMPC along with System-ID.
2. Automated history matching, and in particular the use of Ensemble Kalman Filter (EnKF), has shown to provide models with good matching (past production history) and prediction capabilities, but do not result in parameters with a much geological sense. This is to say that the input-output behavior of the reservoir model is consistent to what is expected as far as production is concerned, but physically they do not represent what the geologist's may believe is a good model. From a system theoretical point of view this is adequate as connecting blocks with the correct input-output description is what

makes sense. Therefore, there should be a way of incorporating geological properties to automated history matching in as seamless manner.

3. Reduced-order models have been shown to produce reasonable approximations to the full and complex reservoir models. Thus, complex models usually have counterparts with much smaller state and parameters dimensions. This is to say that one needs to understand how much the complexities will play a role in the input-output behavior of such models. From a system theoretical point of view, controllability and observability are of central issue, and, in general, the petroleum engineering community has not paid much attention to such properties.

4. Convince the production managers that the operation of the reservoir should be guided not only by experience, but also from “smart” decisions resulted from the closed-loop optimization. The idea is not to completely remove the human element from the loop, but also to let him have the upper hand and the help required on the decision-making process. In several occasions, as pointed out in the literature, short term and long term production can be adjusted to maximize production or to maximize economic objectives, even though at times they may sound contradictory one to another. For instance, one may start producing at a slower pace, so that over the life time of the reservoir we can recover larger amounts of oil and in turn, meet financial or production targets. Thus, better ways of demonstrating the feasibility of the closed-loop system needs to be well thought out.

REFERENCES

- [1] Ertekin, T., Abou-Kassem, J. H., and King, G. R., 2001, *Basic Applied Reservoir Simulation*, 10th ed., SPE Textbook Series, Richardson, TX.
- [2] Jansen, J. D., Bosgra, O. H., and Hof, V. D., 2008, “Model-Based Control of Multiphase Flow in Subsurface Oil Reservoirs,” *Journal of Process Control*, **21**, pp.132-139.
- [3] Dorf, R., and Bishop, R.H., 2010, *Modern Control Systems*, 11th ed., E Prentice Hall, NJ.
- [4] Gildin, E., and Wheeler, M. F., 2008, “Optimal Subsurface Flow Management Using Model Predictive Control Techniques,” *Proceedings of the European Conference on the Mathematics of Oil Recovery*, Bergen, Norway, Aug. 12–15, Paper No. DETC 909/DAC 9185.
- [5] Jansen, J. D., 2009, “Closed Loop Reservoir Management,” *Proceedings of the SPE Reservoir Simulation Symposium*, Woodlands, TX, Apr. 10-14, Paper No. SPE 106242.
- [6] Wang, C., and Reynolds, A.C., 2007, “Production Optimization in Closed-Loop Reservoir Management,” *Proceedings of the SPE Annual Technical Conference and Exhibition*, Anaheim, CA, Paper No. SPE 106352.
- [7] Brouwer, D. R., and Jansen, J. D., 2002, “Dynamic Optimization of Waterflooding with Smart Wells Using Optimal Control Theory,” *Proceedings of the European Petroleum Conference*, Aberdeen, Scotland, UK, Paper No. SPE 78278.

- [8] Brouwer, D. R., 2004, "Improved Reservoir Management Through Optimal Control and Continuous Model Updating," Proceedings of the SPE Annual Technical Conference and Exhibition, Houston, TX, Paper No. SPE 90149.
- [9] Evensen, G., 2009, *Data Assimilation. The Ensemble Kalman Filter*, 2nd ed., Springer, Berlin.
- [10] Gildin, E., Klie, H., Wheeler, M.F., Rodriguez, A., and Bishop, R. H., 2008, "Projection-Based Approximation Methods for the Optimal Control of Smart Fields," Proceedings of the European Conference of the Mathematics of Oil Recovery, Amsterdam, Netherlands, Aug. 10–14, Paper No. DETC 989/DAC 9785.
- [11] Cardoso, M. A., and Durlofsky, L. J., 2010, "Use of Reduced-Order Modeling Procedures for Production Optimization," Proceedings of the SPE Reservoir Simulation Symposium, Woodlands, TX, Paper No. SPE 91254.
- [12] Heijn, T., Markovinovic, R., and Jansen, J. D., 2004, "Generation of Low-Order Reservoir Models Using System-Theoretical Concepts," SPE Journal, **9**, pp. 102-119.
- [13] Doren, V. J., Markovinovic, R., and Jansen, J. D., 2004, "Reduced-Order Optimal Control of Waterflooding Using POD," Proceedings of the European Conference on the Mathematics of Oil Recovery, Cannes, France, Aug. 12–15, Paper No. DETC 805/DAC 9074.
- [14] Antoulas, A.C., 2005, *Approximation of Large-Scale Dynamical Systems*, SIAM, Natick, Philadelphia.

- [15] Zhou, K., Doyle, J. C., and Glover, K., 1996, *Robust and Optimal Control*, Prentice Hall, Englewood Cliffs, NJ.
- [16] Overschee, V. P., and De Moor, B. L. R., 1993, "Subspace algorithms for the Stochastic Identification Problem," *Automatica*, **29**, pp. 649 – 660.
- [17] Overschee, V. P., and De Moor, B. L. R., 1996, *Subspace Identification for Linear Systems: Theory, Implementation, Application*, Kluwer Academic Publishers, NJ.
- [18] Gildin, E., Lopez, T. J., 2011, "Closed-Loop Reservoir Management: Do we need complex models," Proceedings of the SPE Digital Energy Symposium, Woodlands, TX, Apr. 19-21, Paper No. SPE 144336.
- [19] Aziz, K., and Settari, A., 1979, *Petroleum Reservoir Simulation*, Applied Science Publishers, London.
- [20] Peaceman, D.W., 1977, *Fundamentals of Numerical Reservoir Simulation*, Elsevier Applied Scientific Publishing Company, London.
- [21] Maciejowski, J.M., 2002, *Predictive Control with Constraints*, Prentice-Hall, Englewood Cliffs, NJ.
- [22] Gopinath, B., 1969, "On the Identification of Linear Time-Invariant Systems from Input-Output Data," *The Bell System Technical Journal*, **48**, pp. 1101 – 1113.
- [23] Willems, J., 1986, "From Time Series to Linear Systems," *Automatica*, **22**, pp. 561 – 580.
- [24] Willems, J., 1987, "From Time Series to Linear Systems", *Automatica*, **23**, pp. 87 – 115.

- [25] De Moor, B. L. R., 1988, “Mathematical Concepts and Techniques for Modeling of Static and Dynamic Systems,” PhD thesis, Department of Electrical Engineering, Katholieke Universiteit Leuven, Netherlands.
- [26] Moonen, M., DeMoor, B. L. R., Vandenberghe, L., and Vandewalle, J., 1989, “On and off-line identification of linear state space models,” *International Journal of Control*, **49**, pp. 219 – 232.
- [27] Rezapour, A., 2009, “Improved Waterflooding Performance Using Model Predictive Control,” Master of Science Thesis, Department of Systems and Control, Delft University of Technology, Netherlands.

VITA

Thomas Jai Lopez was born to Thomas Joseph Lopez and Filomina Joseph in United Arab Emirates (U.A.E). He pursued his primary education in Sharjah Indian School, U.A.E. He obtained his Bachelor of Engineering degree in mechanical engineering from Birla Institute of Science and Technology, U.A.E, with a first class, in the year 2009.

Thomas Jai Lopez was admitted into the master's program in Fall 2009, with the Petroleum Engineering Department, Dwight Look College of Engineering at Texas A&M University. He joined the Reservoir Simulations and Controls group with Dr. Eduardo Gildin as his research advisor in the spring semester. He joined Flowserve Corporation as an R&D Engineer in May 2011.

He pursued his research in the field of Reservoir Simulation under the guidance of Dr. Eduardo Gildin and his committee members Dr. Akhil Datta Gupta and Dr. Wong-jong Kim. He received his M.S. degree in Petroleum Engineering in December 2011.

Jai's permanent address and Email ID are:

3123 TAMU,

College Station, TX 77843- 3123, USA.

thomas_jai_lopez@yahoo.com